

---

# Oversmoothing as Loss of Sign: Towards Structural Balance in Graph Neural Networks

---

Jiaqi Wang<sup>1</sup> \*   Xinyi Wu<sup>2\*</sup>   James Cheng<sup>1</sup>   Yifei Wang<sup>3</sup>

<sup>1</sup>The Chinese University of Hong Kong   <sup>2</sup>MIT IDSS & LIDS   <sup>3</sup>MIT CSAIL  
 {jqwang23, jcheng}@cse.cuhk.edu.hk   {xinyiwu,yifei\_w}@mit.edu

## Abstract

Oversmoothing is a common issue in graph neural networks (GNNs), where node representations become excessively homogeneous as the number of layers increases, resulting in degraded performance. Various strategies have been proposed to combat oversmoothing in practice, yet they are based on different heuristics and lack a unified understanding of their inherent mechanisms. In this paper, we show that three major classes of anti-oversmoothing techniques can be mathematically interpreted as message-passing over signed graphs comprising both positive and negative edges. By analyzing the asymptotic behavior of signed graph propagation, we demonstrate that negative edges can repel nodes to a certain extent, providing deeper insights into how these methods mitigate oversmoothing. Furthermore, our results suggest that the structural balance of a signed graph—where positive edges exist only within clusters and negative edges appear only between clusters—is crucial for clustering node representations in the long term through signed graph propagation. Motivated by these observations, we propose a solution to mitigate oversmoothing with theoretical guarantees—**Structural Balance Propagation (SBP)**, by incorporating label and feature information to create a structurally balanced graph for message-passing. Experiments on nine datasets against twelve baselines demonstrate the effectiveness of our method, highlighting the value of our signed graph perspective.

## 1 Introduction

Graph neural networks (GNNs) are a powerful framework for processing graph-structured data across a wide range of applications, such as drug discovery, recommender systems and social networks [3, 4, 12, 15, 21, 27, 39]. Most GNN models follow the *message-passing* paradigm, where node features are computed by recursively aggregating information from neighboring nodes along the edges [25, 43, 46, 50]. Despite notable advancements, oversmoothing remains an issue for deploying GNNs in practice, characterized by the convergence of all node features to a common value when stacking a substantial number of GNN layers [5, 26, 34, 47].

Several strategies [10, 28, 29, 31, 35, 41] have been developed to mitigate oversmoothing in GNNs, including normalization layers [1, 2, 22, 52], random edge dropping [18], and residual connections [9, 17, 19, 30, 49]. However, these methods arise from different motivations and lack a unified framework for comparison and analysis, making it unclear why they succeed or fail on specific homophilic or heterophilic graphs and explaining their inefficacy in deep-layer regimes [32, 36, 48].

In this paper, we introduce a signed graph perspective to theoretically analyze existing anti-oversmoothing methods, categorizing eight empirically effective approaches [14, 19, 22, 24, 30, 37, 49, 52] into three major groups. Our analysis reveals that all these methods can be mathematically

---

\*Equal contribution.

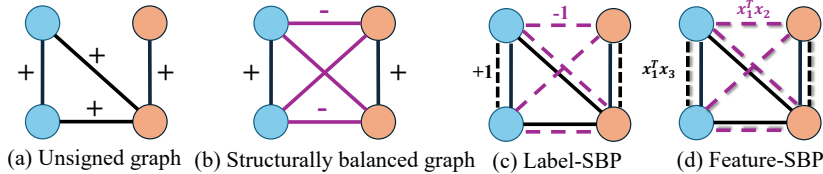


Figure 1: Illustration of different graph structures, edge types used in this work and our method, SBP. Blue and orange circles represent nodes from class 1 and class 2, respectively. Solid lines indicate actual edges, while dashed lines denote constructed edges. Positive and negative edges are represented by black and purple lines, respectively. Let  $x_i$  be the node features for node  $i$ . (a) Unsigned graph with all positive edges. (b) Structurally balanced graph with positive edges within clusters and negative edges between clusters. (c) Label-SBP, which adds negative edges between classes and positive edges within classes. (d) Feature-SBP, which adds edges based on node feature similarities. Here, we assume the underlying graph is homophilic, meaning that node features in the same class are similar. This results in adding positive edges within classes and negative edges between classes.

interpreted as message-passing over a signed graph with different design choices, where negative edges induce repulsion among neighboring nodes, thereby mitigating oversmoothing.

This observation not only highlights how these techniques mitigate oversmoothing through a unified signed graph perspective but also motivates a deeper exploration into the asymptotic behavior of signed graph propagation. Our theoretical analysis suggests that while negative edges can partially disperse nodes and thus help mitigate oversmoothing, message-passing over an arbitrary signed graph would inevitably either converge or diverge over a large number of propagation steps (Theorem 4.1). To address this, we introduce the *structural balance graph*, characterized by a distinctive distribution of positive and negative edges, serving as an ideal condition for controlling the asymptotic behavior of signed graph propagation. As illustrated in Figure 1(b), a structurally balanced graph consists of clusters where only positive edges exist within each cluster and only negative edges exist between clusters. Under signed graph propagation in such a graph, nodes within the same cluster converge to a shared value, while different clusters repel each other to have distinct values (Theorem 4.3). This long-term behavior effectively manages oversmoothing within clusters while simultaneously preserving inter-cluster separation, thereby enhancing node classification accuracy in the long run.

Motivated by our structural balance analysis, we introduce **Structural Balance Propagation (SBP)**, a method for constructing a structurally balanced graph to facilitate signed propagation. Specifically, we propose **Label-SBP**, which assigns positive edges between nodes of the same class and negative edges between nodes of different classes, without introducing additional learnable parameters (Figure 1(c)). This is achieved by preserving the original unsigned graph as the positive graph and leveraging the training labels to construct the negative graph. We show that as the training ratio increases, Label-SBP progressively approximates a structurally balanced graph (Proposition 4.7). To handle scenarios with limited ground truth information, we further introduce a feature-induced variant, **Feature-SBP** (Figure 1(d)). Instead of relying on labels, Feature-SBP constructs the negative graph based on node similarities, enabling its applicability in label-scarce settings.

#### Our main contributions are summarized as follows:

- We present a signed graph perspective to unify three major classes of anti-oversmoothing techniques, demonstrating that they all implicitly involve adding negative edges to the original graph. This perspective offers a unifying framework, shedding light on the underlying mechanisms of these techniques and the role of signed edges in mitigating oversmoothing.
- We introduce **Structural Balance Propagation (SBP)** to alleviate oversmoothing with theoretical guarantees. To quantify the level of structural balance in a signed graph, we propose a novel metric, structural imbalance degree (*SID*). Leveraging both theoretical insights and *SID*, we reveal that existing anti-oversmoothing techniques fail to achieve structural balance due to the improper distribution of signs, which explains their inefficacy in consistently combating oversmoothing over a large number of propagation steps.
- Motivated by the desirable asymptotic behavior of signed graph propagation over structurally balanced graphs, we propose Label-SBP and Feature-SBP, which explicitly design negative edges to enhance the structural balance of the signed graph. Experiments on nine datasets demonstrate that SBP consistently improves node classification accuracy in both homophilic and heterophilic settings, validating the effectiveness of SBP and the value of our signed graph perspective.

Table 1: The mathematically equivalent raw normalized positive and negative adjacency matrices in signed graph propagation of various anti-oversmoothing methods.

Method	Characteristic	Positive $\hat{A}^+$	Negative $\hat{A}^-$
GCN	$K$ -layer graph convolutions	$\hat{A}$	0
SGC	$K$ -layer linear graph convolutions	$\hat{A}$	0
BatchNorm	Normalized with column means and variance	$\hat{A}$	$\mathbb{1}_n \mathbb{1}_n^T / n \hat{A}$
PairNorm	Normalized with the overall means and variance	$\hat{A}$	$\mathbb{1}_n \mathbb{1}_n^T / n \hat{A}$
ContraNorm	Uniformed norm derived from contrastive loss	$\hat{A}$	$(X X^T) \hat{A}$
DropEdge	Randomized augmentation	$\hat{A}$	$\hat{A}_m$
Residual	Last layer connection	$\hat{A}$	$I$
APPNP	Initial layer connection	$\sum_{i=0}^{k+1} \alpha^i \hat{A}^i$	$\alpha \sum_{j=0}^k \alpha^j \hat{A}^j$
JKNET	Jumping to the last layer	$\sum_{i=0}^k \alpha^i \hat{A}^i + \hat{A}^{k+1}$	$\sum_{j=0}^k \alpha^j \hat{A}^j$
DAGNN	Adaptively incorporating different layer	$\sum_{i=0}^k \alpha^i \hat{A}^i + \hat{A}^{k+1}$	$\sum_{j=0}^k \alpha^j \hat{A}^j$
Feature-SBP (ours)	Label-induced negative graph	$\hat{A}$	$\text{softmax}(A^+)$
Label-SBP (ours)	Feature-induced negative graph	$\hat{A}$	$\text{softmax}(A^+)$

## 2 Background

**Notations.** We represent an unsigned undirected graph with  $n$  nodes by  $\mathcal{G} = (A, X)$ , where  $A \in \{0, 1\}^{n \times n}$  denotes the adjacency matrix and  $X \in \mathbb{R}^{n \times d}$  is the node feature matrix. For node  $i, j \in \{1, 2, \dots, n\}$ ,  $A_{i,j} = 1$  if and only if node  $i, j$  are connected by an edge in  $\mathcal{G}$  and  $X_i \in \mathbb{R}^d$  represents the features of node  $i$ . We let  $\mathbb{1}_n$  be the all-one vector of length  $n$  and  $D = \text{diag}(A \mathbb{1}_n)$  be the degree matrix of  $\mathcal{G}$ . In this paper, we extend  $\mathcal{G}$  to the signed graph  $\mathcal{G}_s = \{A^+, A^-, X\}$  where  $A^+, A^- \in \{0, 1\}^{n \times n}$  are the positive and negative adjacency matrices with the degree matrix  $D_+ = \text{diag}(A^+ \mathbb{1}_n)$  and  $D_- = \text{diag}(A^- \mathbb{1}_n)$ , respectively.

**Unsigned and signed graph propagation.** A unsigned graph propagation using the row normalized adjacency matrix  $\hat{A} = D^{-1}A$  takes the form  $X' = \sigma(\hat{A}X)$ , with the nonlinear activation function  $\sigma(\cdot)$  and the learnable weight  $W$ . In this paper, our theoretical analysis focuses on the simplified linear GNN model following Wu et al. [46, 47] by letting  $\sigma(x) = x$ . For convenience, we let  $W^* = W^{(0)}W^{(1)} \dots W^{(K-1)}$  where  $W^{(k)}$  is a learnable weight matrix in the  $k$ -th layer. Following Derr et al. [13], Shi et al. [40], we define the signed graph propagation under the linear GNN as follows:

$$X^{(k+1)} = (1 - \alpha + \beta)X^{(k)} + \alpha \hat{A}^+ X^{(k)} - \beta \hat{A}^- X^{(k)}, \quad (1)$$

$$X^{(0)} = X, \quad X_{out} = X^{(K)}W^*, \quad (2)$$

where  $\hat{A}^+ = D_+^{-1}A^+$  and  $\hat{A}^- = D_-^{-1}A^-$  are the positive and negative row normalized adjacency matrices,  $\alpha, \beta > 0$  are the parameters controlling the strength of the propagation over the positive and negative graphs, respectively, and  $X_{out}$  is the resulting  $K$ -th layer output. Note that the crucial difference between the positive and negative graph lies in the sign preceding their adjacency matrices. When  $\beta = 0, \alpha = 1$ , (1) would correspond to the conventional (unsigned) graph propagation.

## 3 A Signed Graph Perspective on Existing Oversmoothing Countermeasures

In this section, we revisit three popular types of anti-oversmoothing methods and reinterpret them through the lens of signed graph propagation in the form of (1). We find that all of these methods can be attributed to some kind of signed graph design  $\mathcal{G}_s$  by introducing positive and negative edges to the original graph. We summarize eight specific methods with their corresponding positive and negative graphs in Table 1.

### 3.1 Normalization Techniques

Normalization operates the node features after each message-passing step by centering them with zero mean and unit variance (up to a scale) with different strategies. A few representative methods include BatchNorm [24], PairNorm [53], and ContraNorm [22], where PairNorm and ContraNorm were proposed specifically to address the oversmoothing issue in GNNs. Further details on these methods are provided in Appendix D. Despite the differences in motivation and implementation, all

the three normalization methods can be seen as a signed graph propagation with different designs of the negative graph:

**Theorem 3.1** *BatchNorm, PairNorm and ContraNorm can be interpreted as signed graph propagation defined in (1), sharing the same raw normalized positive adjacency matrix  $A^+ = \hat{A}$  while having different raw normalized negative adjacency matrices transformed from  $\hat{A}^+$ , that is,  $\hat{A}^- = \frac{\mathbf{1}_n \mathbf{1}_n^T}{n} \hat{A}$  for BatchNorm and PairNorm, and  $\hat{A}^- = (XX^T)\hat{A}$  for ContraNorm.*

The result shows that PairNorm shares the same fixed positive and negative graphs (up to scale) as BatchNorm. In contrast, ContraNorm extends the negative graph to an adaptive one based on similarities in node features.

### 3.2 Augmentation-Based Methods

Node or edge dropping [37] is another popular type of method to combat oversmoothing. In particular, we denote  $A_m \in \{0, -1\}^{n \times n}$  where  $(A_m)_{i,j} = 1$  if the edge  $\{i, j\}$  is dropped and otherwise 0. Then the signed graph induced by (randomly) dropping edges can be formulated as  $\mathcal{G}_{drop} = \{A, A_m, X\}$ . The negative adjacency matrix  $A_m$ , while created through random generation, effectively helps alleviate oversmoothing in practice.

### 3.3 Residual Connections

Besides normalization layers and edge-dropping, residual connections can also be seen through the lens of signed graph propagation. Based on different combinations of layers in this class, we provide analysis for the following three types of residual connections: First, the standard residual connection [8, 44], which directly combines the previous and the current layer features together. Another type combines the current layer features together with the initial features, such as APPNP [19] or GCNII [9]. In addition to combining with the previous or the initial layer features, there is a third type of residual connections which integrates intermediate layer features, such as JKNET [49] and DAGNN [30]. More details about these methods can be found in Appendix D.2. Formally, we establish the following result that these three types of residual connections can all be seen as signed graph propagation:

**Theorem 3.2** *With  $\hat{A}^+ = \hat{A}$  and  $\hat{A}^- = I$ , the standard residual connections follows the signed graph propagation (1). With  $\hat{A}^+ = \sum_{i=0}^{k+1} \alpha^i \hat{A}^i$  and  $\hat{A}^- = \alpha \sum_{j=0}^k \alpha^j \hat{A}^j$ , APPNP follows the signed graph propagation (1). With  $\hat{A}^+ = \sum_{i=0}^{k-1} \alpha^i \hat{A}^i + \hat{A}^k$  and  $\hat{A}^- = \sum_{j=0}^{k-1} \alpha^j \hat{A}^j$ , JKNET and DAGNN follows the signed graph propagation (1).*

**Discussion.** In summary, we establish a unifying perspective in which normalization, edge dropping, and residual connections can all be interpreted as instances of signed graph propagation, even though this structure is not explicitly recognized. Notably, for these methods, while their positive adjacency matrices typically reflect the original graph structure, the negative adjacency matrices are often constructed heuristically. As a result, the interaction between signed graph structures and node feature dynamics remains insufficiently understood motivating a systematic theoretical analysis of the asymptotic behaviors of signed graph propagation.

## 4 Structural Balance Propagation

In this section, we begin by analyzing the asymptotic behavior of signed graph propagation. Our findings suggest that *structural balanced graphs* exhibit controllable long-term asymptotic behavior, making them effective in mitigating oversmoothing with theoretical guarantees. Building on this insight, we propose two methods, Label/Feature-SBP, and introduce a metric *SID* to quantify the structural imbalance of different anti-oversmoothing methods approaches. Our theoretical analysis and this metric help identify the underlying reasons for the inefficacy of previous methods in addressing oversmoothing in the deep-layer regime.

#### 4.1 Asymptotic Behavior of Signed Graph Propagation

For simplicity, we initially focus on individual nodes and their interactions via positive and negative edges with other nodes [40]. This analysis leads us to convert the matrix-based signed graph propagation in (1) to the equivalent node level as follows:

$$X_i^{(k+1)} = (1 - \alpha + \beta)X_i^{(k)} + \frac{\alpha}{D_i^+} \sum_{j \in N_i^+} X_j^{(k)} - \frac{\beta}{D_i^-} \sum_{j \in N_i^-} X_j^{(k)}, \quad (3)$$

where  $N_i^+$  and  $N_i^-$  represent the set of positive and negative neighbors for node  $i$ ,  $D_i^+$  and  $D_i^-$  represents the degree for the positive and negative adjacency matrices, respectively. Note that while (3) is defined for a single node  $X_i^{(k+1)}$ , it can be naturally extended to the whole matrix  $X^{(k+1)}$  by applying the same iterative process to each node.<sup>2</sup>

We first show that insufficient repulsion among nodes can still result in oversmoothing, even under the signed graph propagation. Conversely, excessive repulsion can also be detrimental, causing node representations to diverge and hindering overall performance.

**Theorem 4.1** *Suppose that the signed graph  $\mathcal{G}_s$  where  $A^+$  represents a connected graph and  $X_i^{(k)}$  represents the value of node  $i$  after  $k$  propagation steps under (3). Then for any  $0 < \alpha < 1/\max_{i \in X} D_i^+$ , there exists a critical value  $\beta_* \geq 0$  for  $\beta$  such that if  $\beta < \beta_*$ , then we have  $\lim_{k \rightarrow \infty} X_i^{(k)} = \sum_{j=1}^n X_j^{(0)}/n$  for all initial values  $X^{(0)}$ ; if  $\beta > \beta_*$ , then  $\lim_{k \rightarrow \infty} \|X^{(k)}\| = \infty$  for almost all initial values w.r.t. Lebesgue measure.*

**Repulsion strength  $\beta$  matters.** The parameter  $\beta$  represents the strength of repulsion between nodes, acting as a counterforce to the homogenizing trend of oversmoothing and preserving the heterogeneity of node features within the network. Theorem 4.1 suggests that if the weight  $\beta$  assigned to negative edges is small—particularly when  $\beta = 0$ , corresponding to the standard unsigned graph propagation—node features will inevitably converge to a common value, resulting in oversmoothing. However, if  $\beta$  is too large, the node features will diverge instead of converging, potentially causing numerical issues [45].

**Problem of previous anti-oversmoothing methods.** Normalization layers generate negative graphs through linear transformations of the original adjacency matrix, augmentation methods randomly mask elements by setting them to zero, and residual connection methods combine different orders of the adjacency matrix linearly. However, none of these methods explicitly consider the repulsion strength  $\beta$  or the interaction between positive and negative graphs. As a result, their induced signed graphs  $\mathcal{G}_s$  effectively remain as variants of the original adjacency matrix, causing the repulsion strength to depend implicitly on the initial graph structure or the positive weight,  $\alpha$ . This implicit dependency limits their effectiveness in mitigating oversmoothing, regardless of whether the graph is homophilic or heterophilic.

#### 4.2 Asymptotic Behavior of Propagation over Structurally Balanced Graphs

Given the limitations of previous methods, where attraction implicitly influences repulsion, we shift our focus to separately examining the distinct roles of positive and negative graphs. To this end, we present the *structural balance graph*, which accounts for the distribution of signed edges across different clusters and exhibits controllable asymptotic behavior under signed graph propagation. Formally, following Cartwright and Harary [7], Shi et al. [40], we define structurally balanced graphs as follows.

**Definition 4.2 (Structurally Balanced Graph)** *A signed graph  $\mathcal{G}_s$  is called **structurally balanced** if there is a partition of the node set into  $V = \tilde{V}_1 \cup \tilde{V}_2$  with  $\tilde{V}_1$  and  $\tilde{V}_2$  being nonempty and mutually disjoint, where any edge between the two node subsets  $\tilde{V}_1$  and  $\tilde{V}_2$  is negative, and any edge within each  $\tilde{V}_i$  is positive.*

The structural balance property partitions the graph into two disjoint node groups, ( $\tilde{V}_1$  and  $\tilde{V}_2$ ), where intra-group and inter-group edges are separated based on their signs, as illustrated in Figure 1(b).

<sup>2</sup>For additional results into the connections between node-level dynamics, the whole graph  $\mathcal{G}_s$ , and the oversmoothing, see Appendix G.

Moreover, to address the divergence of node representations caused by excessive repulsion, we introduce a bounded function  $\mathcal{F}(\cdot)_c$  that constrains node features to a maximum value  $c$ , transforming unbounded divergence into a controlled scale. We characterize the asymptotic behavior of propagation over structurally balanced graphs as follows:

**Theorem 4.3** *Assume that node  $i$  is connected to node  $j$  and  $X_i^{(k)}$  represents the value of node  $i$  after  $k$  propagation steps in (3).  $\mathcal{F}(z)_c$  is a bounded function satisfying: if  $z < -c$ ,  $\mathcal{F}(z)_c = -c$ ; if  $z > c$ ,  $\mathcal{F}(z)_c = c$ ; if  $-c < z < c$ ,  $\mathcal{F}(z)_c = z$ . Let  $\theta = \alpha$  if the edge  $\{i, j\}$  is positive and  $\theta = -\beta$  if the edge  $\{i, j\}$  is negative. Consider the constrained signed propagation update:*

$$X_i^{(k+1)} = \mathcal{F}_c((1 - \theta)X_i^{(k)} + \theta X_j^{(k)}). \quad (4)$$

Let  $\alpha \in (0, 1/2)$ . Assume that  $\mathcal{G}_s$  is a structurally balanced complete graph under the partition  $V = \tilde{V}_1 \cup \tilde{V}_2$ . When  $\beta$  is sufficiently large, we have that

$$\mathbb{P}\left(\lim_{k \rightarrow \infty} X_i^{(k)} = c, i \in \tilde{V}_1; \lim_{k \rightarrow \infty} X_i^{(k)} = -c, i \in \tilde{V}_2\right) = 1. \quad (5)$$

Theorem 4.3 shows that if the graph is structurally balanced and the signed graph propagation is constrained with  $\mathcal{F}_c$ , node features will converge to their respective group-specific values asymptotically under the signed graph propagation defined in (1). Furthermore, different groups will repel each other to have distinct values, even asymptotically. Based on the insight in [48], this implies that structurally balanced graphs would be an ideal case for provably addressing oversmoothing through signed graph propagation.

**Remark 4.4** *We can generalize the two distinct groups in the above result to a generic number of distinct groups by introducing a more general notion, weakly structural balance. See a detailed discussion in Appendix H.*

### 4.3 Design Structural Balance Propagation for GNNs

Previously, we have established the asymptotic behavior of signed graph propagation on structurally balanced graphs, demonstrating its ability to provably alleviate oversmoothing. Building on this theoretical insight, we propose **Structural Balance Propagation (SBP)** to enhance structural balance in signed graphs. Specifically, we introduce two simple yet effective methods, **Label-SBP** and **Feature-SBP**, which leverage label and feature information, respectively, to construct negative graphs. By strategically incorporating these negative edges, our approach improves structural balance, ensuring more stable and expressive node representations under signed graph propagation while effectively combating oversmoothing.

**Label-SBP.** For simplicity, we let positive adjacency matrix to be the original adjacency matrix  $\hat{A}^+ = \hat{A}$ , aligning with many prior anti-oversmoothing methods summarized in Table 1. We then construct the negative adjacency matrix  $A_l^-$  based on training labels to achieve an overall structurally balanced graph, thereby mitigating across-label oversmoothing. Specifically, we repel nodes from different classes by assigning value 1, attract nodes from the same class by assigning value  $-1$ , and neither repel nor attract nodes by assigning value 0 when labels are unknown in the negative adjacency matrix:

$$(A_l^-)_{ij} = \begin{cases} 1 & \text{if } y_i \neq y_j, \\ -1 & \text{if } y_i = y_j, \\ 0 & \text{otherwise,} \end{cases} \quad (6)$$

where  $y_i$  is the ground truth label for node  $i$ . We prove that under certain conditions Label-SBP can construct a structurally balanced graph in Section 4.4. Nonetheless, we further propose a variant of our method that estimates the negative adjacency matrix based on feature similarities, mitigating the performance degradation of Label-SBP in label-scarce scenarios.

**Feature-SBP.** In addition to the label signal, we can also leverage the similarity matrix derived from the node features to create the negative matrix  $A_f^-$ . Formally, the negative adjacency matrix  $A_f^-$  induced by Feature-SBP is defined as:

$$A_f^- = -X^{(0)}X^{(0)\top}. \quad (7)$$

Table 2: *SID* on CSBM (Contextual Stochastic Block Model ) with different methods. We set the two class means  $u_1 = -1$  and  $u_2 = 1$  respectively, the number of nodes  $N = 100$ , intra-class edge probability  $p = 2 \log 100/100$  and inter-class edge probability  $q = \log 100/100$ .

Method	$\mathcal{P}_\downarrow$	$\mathcal{N}_\downarrow$	<i>SID</i> $_\downarrow$
DropEdge	92.62	100.00	96.31
Residual	90.87	100.00	95.44
GCN/SGC	89.87	100.00	94.94
APPNP	0.00	100.00	50.00
JKNET	0.00	100.00	50.00
DAGNN	0.00	100.00	50.00
BatchNorm	89.87	4.56	47.22
PairNorm	89.87	4.56	47.22
ContraNorm	89.87	4.56	47.22
Feature-SBP (ours)	89.87	4.56	47.22
Label-SBP (ours)	32.46	36.16	34.31

While the use of the node feature as the repulsion signal may not be as precise as the Label-SBP, it can make use of all node features and thus can be adjusted to the test set, improving the overall structural balance property of the graph.

**Implementation details.** We implement the constrained function  $\mathcal{F}_c$  in Theorem 4.3 by Layer-Norm [2], following Guo et al. [22]. To avoid numerical instability for repeated message-passing, we ensure that the sum of the coefficients combining the node representations  $X^{(k)}$  and the node representations updates by our SBP remains 1. Additionally, we apply the softmax function to the negative matrix, resulting in  $\hat{A}^- = \text{softmax}(A^-)$ . As a result, Label/Feature-SBP can be written as:

$$X^{(k+1)} = (1 - \lambda)X^{(k)} + \lambda \left( \alpha \hat{A}^+ X^{(k)} - \beta \text{softmax}(A_l^- \text{ or } A_f^-) X^{(k)} \right).$$

**Scalability on large-scale graphs.** To reduce the memory consumption of the potentially dense negative adjacency in large-scale graphs, we introduce a modified version Label-SBP-v2 by only removing edges when pairs of nodes belong to different classes. This approach allows Label-SBP-v2 to eliminate the computational overhead of the negative graph, preserving the sparsity of large-scale graphs. For Feature-SBP, as the number of nodes  $n$  increases, the complexity of its matrix operation grows quadratically, i.e.,  $\mathcal{O}(n^2d)$ . To address this, we reorder the matrix multiplication from  $-XX^\top \in \mathbb{R}^{n \times n}$  to  $-X^\top X \in \mathbb{R}^{d \times d}$ . This preserves the distinctiveness of node representations across the feature dimension, rather than across the node dimension as in the original node-level repulsion. Formally, Feature-SBP-v2 can be expressed as:

$$X^{(k+1)} = (1 - \lambda)X^{(k)} + \lambda \left( \alpha \hat{A}^+ X^{(k)} - \beta X^{(k)} \text{softmax}(-X^{(0)\top} X^{(0)}) \right).$$

This transposed alternative has a linear complexity in the number of samples, i.e.,  $\mathcal{O}(nd^2)$ , significantly reducing the computational burden in cases where  $n \gg d$ . More analysis and time complexity experiments are provided in the Appendix L.

#### 4.4 Theoretical analysis of SBP

In this section, we show that our method SBP can create a structurally balanced graph under certain conditions and thus provably alleviate oversmoothing as the number of propagation steps increases. To achieve this, we introduce a metric, *structural imbalance degree* (*SID*), to quantify the level of structural balance in arbitrary signed graph. Specifically, *SID* counts the number of edges that must be changed to achieve the structural balance.

**Definition 4.5 (Structural Imbalance Degree)** For each node  $v$  in a signed graph  $\mathcal{G}_s$  of  $n$  nodes, let  $\mathcal{P}(v)$  denote the subset of nodes that has the same label as  $v$  but connected to  $v$  by a non-positive edge; let  $\mathcal{N}(v)$  denote the subset of nodes that has a different label from  $v$  but connected to  $v$  by a non-negative edge. Then the structural imbalance degree of  $\mathcal{G}$  is defined as  $\text{SID}(\mathcal{G}_s) = \frac{1}{2n} \sum_{v \in \mathcal{G}_s} (|\mathcal{P}(v)| + |\mathcal{N}(v)|)$ .

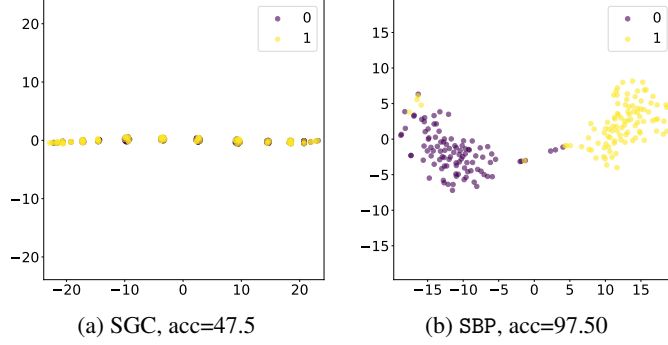


Figure 2: The t-SNE visualization of the node features on the same CSBM setting as Table 2 under Layer=300.

Table 3: Node classification accuracy (%) on 8 datasets and  $H(G)$  refers to the edge homophily level. The best results are marked in blue and the second best results are marked in gray on every layer. Overall SBP performs best in both homophilic and heterophilic datasets.

$H(G)$ Dataset	0.81 Cora	0.74 Citeseer	0.80 PubMed	0.22 Squirrel	0.38 Amazon-ratings	0.21 Texas	0.11 Wisconsin	0.30 Cornell
MLP	48.82 ± 0.98	47.89 ± 1.21	69.20 ± 0.83	32.58 ± 0.19	38.14 ± 0.03	73.51 ± 2.36	70.98 ± 1.18	68.11 ± 2.65
SGC	80.21 ± 0.07	71.88 ± 0.27	76.99 ± 0.38	43.30 ± 0.30	42.83 ± 0.04	45.95 ± 0.00	47.06 ± 0.00	48.11 ± 3.15
GCNII	78.58 ± 0.00	61.66 ± 0.67	75.41 ± 0.00	31.22 ± 0.00	40.10 ± 0.28	63.24 ± 1.34	60.78 ± 0.00	38.38 ± 1.08
$w$ GCN	80.97 ± 0.28	66.21 ± 0.63	76.35 ± 0.38	43.78 ± 0.23	42.65 ± 0.20	49.73 ± 2.16	58.82 ± 0.00	43.24 ± 0.00
BatchNorm	77.90 ± 0.00	60.85 ± 0.09	77.15 ± 0.09	44.22 ± 0.11	39.68 ± 0.01	39.73 ± 1.24	52.94 ± 0.00	46.49 ± 1.08
PairNorm	80.30 ± 0.05	70.83 ± 0.06	77.69 ± 0.26	46.21 ± 0.09	42.30 ± 0.05	51.35 ± 0.00	58.82 ± 0.00	51.35 ± 0.00
ContraNorm	81.60 ± 0.00	72.25 ± 0.08	79.30 ± 0.10	48.63 ± 0.16	42.98 ± 0.04	48.38 ± 4.43	49.61 ± 1.53	48.63 ± 0.16
DropEdge	73.58 ± 2.76	65.63 ± 1.76	74.64 ± 1.37	42.30 ± 0.62	42.30 ± 0.09	59.46 ± 8.11	52.55 ± 4.45	45.95 ± 7.05
Residual	77.81 ± 0.03	71.61 ± 0.17	77.40 ± 0.06	43.63 ± 0.34	42.69 ± 0.03	65.95 ± 1.32	63.73 ± 0.98	61.89 ± 3.91
APPNP	77.78 ± 0.93	67.42 ± 1.31	74.52 ± 0.49	42.15 ± 0.17	42.47 ± 0.03	68.38 ± 4.37	65.10 ± 1.71	64.59 ± 3.30
JKNET	78.20 ± 0.20	66.80 ± 0.33	75.62 ± 0.37	48.16 ± 0.25	42.21 ± 0.05	60.00 ± 2.36	42.55 ± 2.92	39.73 ± 2.72
DAGNN	65.98 ± 1.49	60.04 ± 1.98	72.39 ± 0.90	33.39 ± 0.19	40.61 ± 0.03	61.35 ± 1.73	57.45 ± 1.97	44.87 ± 3.24
Feature-SBP	82.46 ± 0.07	70.63 ± 0.52	77.41 ± 0.21	49.16 ± 0.19	42.31 ± 0.03	78.38 ± 0.00	80.39 ± 0.00	72.97 ± 0.00
Label-SBP	82.90 ± 0.00	73.04 ± 0.10	80.32 ± 0.04	45.60 ± 0.11	42.41 ± 0.02	78.38 ± 0.00	80.39 ± 0.00	70.27 ± 0.00

$SID$  exhibits a fundamental characteristic: it increases as more edge signs deviate from the criteria of a structurally balanced graph, suggesting a higher degree of structural imbalance. Specifically, when the signed graph achieves the structural balance, we can assert that  $SID = 0$  as follows:

**Proposition 4.6** For a structural balanced complete graph  $\mathcal{G}_{sb}$ , we have  $SID(\mathcal{G}_{sb}) = 0$ .

Based on the  $SID$ , we can quantify the degree of structural balance in the equivalent signed graphs induced by anti-oversmoothing methods discussed in the previous section, as shown in Table 2. Our results show that previous anti-oversmoothing methods either remain a high  $SID$  or an imbalance  $\mathcal{P}$  and  $\mathcal{N}$ . In contrast, our methods effectively reduce the  $SID$ , resulting in a more structurally balanced graph, or at least be on par with previous methods. Furthermore, we present the visualization of node features learned by Label-SBP in Figure 2, showing that a lower  $SID$  can indeed lead to higher accuracy even in deeper layers, thus alleviating oversmoothing effectively. We discuss more interesting behaviors about  $SID$  in Appendix I.4.

Besides the empirical observation, we present the following theoretical result which demonstrates that Label-SBP can be guaranteed to achieve a certain level of structure balance:

**Proposition 4.7** Assuming balanced node label classes with  $|Y_1| = |Y_2|$ , a labeled node ratio denoted as  $p$ , and the signed graph  $\mathcal{G}_s^l$  created by Label-SBP, then we have  $SID(\mathcal{G}_s^l) \leq (1 - p)n/2$ .

Proposition 4.7 suggests that Label-SBP constrains  $SID$  linearly with the training ratio  $p$ , indicating that  $SID$  diminishes with an increase in the labeling ratio  $p$ . In particular, it implies that Label-SBP can strictly establish a structurally balanced graph for any graph under the full supervision condition, making the model easier to distinguish nodes with different labels as the number of layers increases:



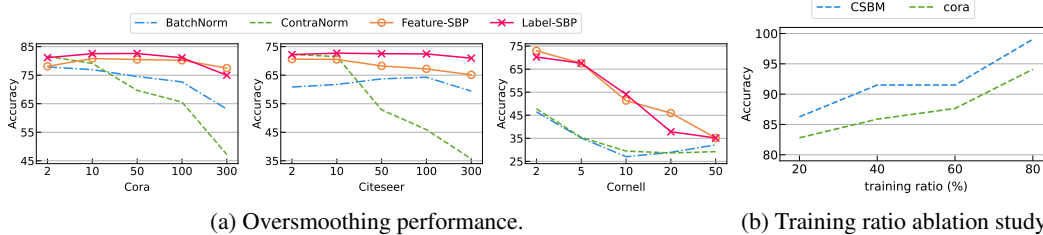


Figure 3: Left is the performance comparison of SBP against Normalization GNNs under various model depths where the X-axis has the number of layers, and the Y-axis has node classification accuracy. Right is the ablation study on Label-SBP where the X-axis indicates the ratio of the training node numbers.

**Theorem 4.8** *Under full supervision ( $p = 1$ ), the signed graph  $\hat{G}_s^l$  induced by Label-SBP achieves  $STD(\hat{G}_s^l) = 0$ . Consequently, under the constrained signed propagation as given by equation 4, nodes from distinct classes will converge towards unique constants.*

$$\mathbb{P} \left( \lim_{k \rightarrow \infty} X_i^{(k)} = c, i \in \tilde{V}_1; \lim_{k \rightarrow \infty} X_i^{(k)} = -c, i \in \tilde{V}_2 \right) = 1. \quad (8)$$

## 5 Experiments

In this section, we conduct a comprehensive evaluation of SBP on various benchmark datasets, including both homophilic and heterophilic graphs. We aim to answer the following three key research questions: **RQ1** How does SBP perform in node classification tasks? **RQ2** How effectively does SBP mitigate oversmoothing? **RQ3** How sensitive, robust, and scalable is SBP?

**Datasets.** We use nine widely-used node classification benchmark datasets (Table 8), where four of them are heterophilic (Texas, Wisconsin, Cornell, Squirrel, and Amazon-rating [36]), and the remaining four are homophilic (Cora [33], Citeseer [20], and Pubmed [6]) including one large-scale dataset (Ogbn-Arxiv [23]). Further information about the datasets and splits are provided in Appendix M.

**Baselines and experiment settings.** We compare the performance of SBP against the following 12 baseline models. 1) **Classic models:** MLP, SGC [46]. 2) **GNNs with normalization:** BatchNorm [24], PairNorm [52] and ContraNorm [22]. 3) **Augmentation-based GNNs:** DropEdge [37]. 4) **GNNs with residual connections:** Residual, APPNP [19], JKNET [49] and DAGNN [30]. 5) **Other baselines:** GCNII [9] and  $\omega$ GCN [17]. For the sake of fair comparison, we do not deploy specific training techniques used in some prior works for benchmarking. All models are trained under the same setting on the pure SGC backbone and we choose the best of scale controller in the range of  $\{0.1, 0.5, 0.9\}$  for ContraNorm, DropEdge, and residual connections. We choose the best of  $\lambda$  in the range of  $\{0.1, 0.5, 0.9\}$ , fix  $\alpha = 1$  and select the best value for  $\beta$  from  $\{0.1, 0.5, 0.9\}$  for SBP. More experiment results with hyperparameter tuning and optimization strategies can be found in Appendix M.

**RQ1: Node classification performance.** In Table 8, we provide the mean of the node classification accuracy along with their corresponding standard deviations across 10 random seeds under the same 2-layer SGC backbone following Wang et al. [44]. Overall, SBP achieves the best performance across 8 datasets in the shallow layers, as Label/Feature-SBP performs the best on 7 out of the 8 datasets.

**RQ2: Anti-oversmoothing analysis.** We further evaluate the robustness of SBP by assessing its performance at deeper model depths:  $K \in \{2, 10, 50, 100, 300\}$  for homophilic datasets and  $K \in \{2, 5, 10, 20, 50\}$  for heterophilic datasets. Figure 3a shows that the performance of Feature/Label-SBP remains relatively stable with varying numbers of layers, achieving its best performance when the model gets deeper. In contrast, the normalization methods considered exhibit a substantial decrease in performance as the number of layers increases, indicating their persistent susceptibility to the oversmoothing problem. Note that we find that for SBP to maintain performance in the heterophilic dataset,  $\beta$  needs to be larger than the uniform range considered in Figure 3a. See Appendix M for the result under larger  $\beta$ , where SBP on deep layers remains  $\approx 60\%$  in Cornell.

**RQ3.1: Sensitivity analysis of training ratio.** As shown in Figure 3b, Label-SBP’s performance on the CSBM and Cora datasets improves as the training ratio increases. Even with a modest training

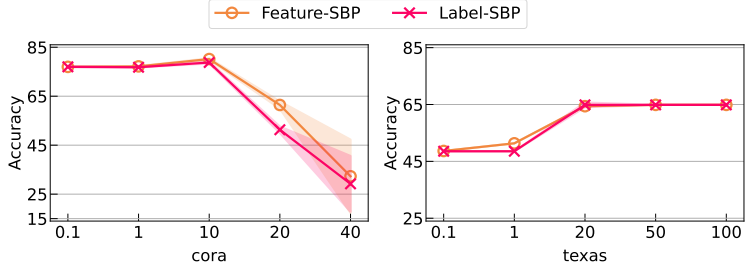


Figure 4: Significance of negative graph weight  $\beta$  on Cora and Texas datasets where we fix the positive graph weight  $\alpha = 1$  and vary a large range of  $\beta$ .

Table 4: Node classification accuracy (%) on the large-scale dataset *ogbn-arxiv*.

Model	#L=2	#L=4	#L=8	#L=16
GCN	67.32 $\pm$ 0.28	67.79 $\pm$ 0.25	65.54 $\pm$ 0.31	59.13 $\pm$ 0.95
BatchNorm	70.14 $\pm$ 0.28	70.93 $\pm$ 0.15	70.14 $\pm$ 0.43	63.24 $\pm$ 1.40
PairNorm	70.48 $\pm$ 0.20	71.59 $\pm$ 0.17	71.24 $\pm$ 0.07	68.92 $\pm$ 0.43
ContraNorm	OOM	OOM	OOM	OOM
DropEdge	64.07 $\pm$ 0.32	63.92 $\pm$ 0.27	60.74 $\pm$ 0.45	52.52 $\pm$ 0.34
Residual	66.90 $\pm$ 0.14	66.67 $\pm$ 0.25	61.76 $\pm$ 0.62	53.25 $\pm$ 0.75
Label-SBP-v2	70.55 $\pm$ 0.22	71.54 $\pm$ 0.18	71.07 $\pm$ 0.28	69.33 $\pm$ 0.59

ratio of 20%, the worst-performing models still achieve an impressive 80% accuracy, while the best models approach 100% accuracy when the training ratio is increased to 80%. This is in line with our theoretical insights that increasing the training ratio leads to more structural balance resulting from our method SBP.

**RQ3.2: Performance under varying graph homophily and heterophily levels.** In order to test the performance of SBP on graphs with arbitrary levels of homophily and heterophily, we conduct an ablation study in the CSBM setting with the controllable homophilic and heterophilic levels following Chien et al. [10]. As shown in Figure 5, Feature/Label-SBP performs best in homophilic graphs when all nodes are effectively attracted to one another, i.e., when the repulsion strength  $\beta$  is small. As  $\beta$  increases, the performance of the model degrades. In contrast, for heterophilic graphs, when the attraction power of the positive graph dominates, SBP achieves only 50% accuracy. As  $\beta$  increases, the negative graph becomes more dominant, and the model’s performance gets significantly better. We observe similar phenomena in the real homophilic and heterophilic graph datasets as shown in Figure 4.

**RQ3.3: Performance on large-scale dataset.** Finally, we conduct an evaluation of SBP on the large-scale *ogbn-arxiv* dataset, and the results are presented in Table 4. Overall, the results demonstrate that Label-SBP-v2 achieves comparable or even superior performance compared to previous normalization methods, particularly in the deep layer setting ( $L = 16$ ). This verifies the empirical superiority and robustness of our proposed signed graph construction in SBP, which effectively leverages the available label information to alleviate oversmoothing, even at scale.

## 6 Conclusion

In this work, we propose a novel unified signed graph perspective by revisiting the concept and theory of signed graphs to study the oversmoothing issue in GNNs. We find that many previous methods alleviating oversmoothing can be seen as implicitly adopting different signed graph designs. Building on this insight, we propose two novel methods, we further propose two novel methods Label-SBP and Feature-SBP, inspired by the structural balance theory. Our work offers new insights from signed graphs, providing a theoretical foundation for analyzing and addressing oversmoothing. This perspective fosters a deeper understanding of the problem and offers guidance for future research in this direction.

## 7 Impact Statement

This paper presents work whose goal is to advance the field of Machine Learning. There are many potential societal consequences of our work, none which we feel must be specifically highlighted here.

### References

- [1] Ameen Ali, Tomer Galanti, and Lior Wolf. Centered self-attention layers. *ArXiv*, 2023.
- [2] Jimmy Lei Ba, Jamie Ryan Kiros, and Geoffrey E Hinton. Layer normalization. *ArXiv*, 2016.
- [3] Peter Battaglia, Razvan Pascanu, Matthew Lai, Danilo Jimenez Rezende, and koray kavukcuoglu. Interaction networks for learning about objects, relations and physics. In *NeurIPS*, 2016.
- [4] Joan Bruna, Wojciech Zaremba, Arthur D. Szlam, and Yann LeCun. Spectral networks and locally connected networks on graphs. In *ICLR*, 2014.
- [5] Chen Cai and Yusu Wang. A note on over-smoothing for graph neural networks. In *ICML Graph Representation Learning and Beyond (GRL+) Workshop*, 2020.
- [6] Kathi Canese and Sarah Weis. PubMed: the bibliographic database. *The NCBI handbook*, 2013.
- [7] Dorwin Cartwright and Frank Harary. Structural balance: a generalization of heider’s theory. *Psychological review*, 1956.
- [8] Ming Chen, Zhewei Wei, Zengfeng Huang, Bolin Ding, and Yaliang Li. Simple and deep graph convolutional networks. In *ICML*, 2020.
- [9] Ming Chen, Zhewei Wei, Zengfeng Huang, Bolin Ding, and Yaliang Li. Simple and deep graph convolutional networks. In *International Conference on Machine Learning*, 2020.
- [10] Eli Chien, Jianhao Peng, Pan Li, and Olgica Milenkovic. Adaptive universal generalized pagerank graph neural network. *arXiv preprint arXiv:2006.07988*, 2020.
- [11] Weilin Cong, Morteza Ramezani, and Mehrdad Mahdavi. On provable benefits of depth in training graph convolutional networks. *ArXiv*, 2021.
- [12] Michaël Defferrard, Xavier Bresson, and Pierre Vandergheynst. Convolutional neural networks on graphs with fast localized spectral filtering. In *NeurIPS*, 2016.
- [13] Tyler Derr, Yao Ma, and Jiliang Tang. Signed graph convolutional networks. In *ICDM*, 2018.
- [14] Tien Huu Do, Duc Minh Nguyen, Giannis Bekoulis, Adrian Munteanu, and Nikos Deligiannis. Graph convolutional neural networks with node transition probability-based message passing and dropout regularization. *ArXiv*, 2020.
- [15] David Kristjanson Duvenaud, Dougal Maclaurin, Jorge Aguilera-Iparraguirre, Rafael Gómez-Bombarelli, Timothy D. Hirzel, Alán Aspuru-Guzik, and Ryan P. Adams. Convolutional networks on graphs for learning molecular fingerprints. In *NeurIPS*, 2015.
- [16] Moshe Eliasof, Eldad Haber, and Eran Treister. Pde-gcn: Novel architectures for graph neural networks motivated by partial differential equations. In *Neural Information Processing Systems*, 2021.
- [17] Moshe Eliasof, Lars Ruthotto, and Eran Treister. Improving graph neural networks with learnable propagation operators. In *International Conference on Machine Learning*, 2022.
- [18] Taoran Fang, Zhiqing Xiao, Chunping Wang, Jiarong Xu, Xuan Yang, and Yang Yang. Dropmessage: Unifying random dropping for graph neural networks. In *AAAI Conference on Artificial Intelligence*, 2022.
- [19] Johannes Gasteiger, Aleksandar Bojchevski, and Stephan Günnemann. Predict then propagate: Graph neural networks meet personalized pagerank. *ArXiv*, 2018.

- [20] C Lee Giles, Kurt D Bollacker, and Steve Lawrence. CiteSeer: An automatic citation indexing system. In *Proceedings of the third ACM conference on Digital libraries*, 1998.
- [21] M. Gori, G. Monfardini, and F. Scarselli. A new model for learning in graph domains. In *IJCNN*, 2005.
- [22] Xiaojun Guo, Yifei Wang, Tianqi Du, and Yisen Wang. ContraNorm: A contrastive learning perspective on oversmoothing and beyond. In *ICLR*, 2023.
- [23] Weihua Hu, Matthias Fey, Marinka Zitnik, Yuxiao Dong, Hongyu Ren, Bowen Liu, Michele Catasta, and Jure Leskovec. Open graph benchmark: Datasets for machine learning on graphs. *arXiv preprint arXiv:2005.00687*, 2020.
- [24] Sergey Ioffe and Christian Szegedy. Batch normalization: Accelerating deep network training by reducing internal covariate shift. In *ICML*, 2015.
- [25] Thomas N. Kipf and Max Welling. Semi-supervised classification with graph convolutional networks. In *ICLR*, 2017.
- [26] Qimai Li, Zhichao Han, and Xiao-Ming Wu. Deeper insights into graph convolutional networks for semi-supervised learning. In *AAAI*, 2018.
- [27] Yujia Li, Daniel Tarlow, Marc Brockschmidt, and Richard S. Zemel. Gated graph sequence neural networks. In *ICLR*, 2016.
- [28] Langzhang Liang, Xiangjing Hu, Zenglin Xu, Zixing Song, and Irwin King. Predicting global label relationship matrix for graph neural networks under heterophily. In *NeurIPS*, 2024.
- [29] Langzhang Liang, Sunwoo Kim, Kijung Shin, Zenglin Xu, Shirui Pan, and Yuan Qi. Sign is not a remedy: Multiset-to-multiset message passing for learning on heterophilic graphs. *arXiv preprint arXiv:2405.20652*, 2024.
- [30] Meng Liu, Hongyang Gao, and Shuiwang Ji. Towards deeper graph neural networks. In *Proceedings of the 26th ACM SIGKDD international conference on knowledge discovery & data mining*, 2020.
- [31] Sitao Luan, Chenqing Hua, Qincheng Lu, Jiaqi Zhu, Mingde Zhao, Shuyuan Zhang, Xiaoming Chang, and Doina Precup. Revisiting heterophily for graph neural networks. *ArXiv*, 2022.
- [32] Yao Ma, Xiaorui Liu, Neil Shah, and Jiliang Tang. Is homophily a necessity for graph neural networks? *arXiv preprint arXiv:2106.06134*, 2021.
- [33] Andrew Kachites McCallum, Kamal Nigam, Jason Rennie, and Kristie Seymore. Automating the construction of internet portals with machine learning. *Information Retrieval*, 2000.
- [34] Kenta Oono and Taiji Suzuki. Graph neural networks exponentially lose expressive power for node classification. In *ICLR*, 2020.
- [35] Jie Peng, Runlin Lei, and Zhewei Wei. Beyond over-smoothing: Uncovering the trainability challenges in deep graph neural networks. In *International Conference on Information and Knowledge Management*, 2024.
- [36] Oleg Platonov, Denis Kuznedelev, Michael Diskin, Artem Babenko, and Liudmila Prokhorenkova. A critical look at the evaluation of gnns under heterophily: Are we really making progress? *arXiv preprint arXiv:2302.11640*, 2023.
- [37] Yu Rong, Wenbing Huang, Tingyang Xu, and Junzhou Huang. Dropedge: Towards deep graph convolutional networks on node classification. *ArXiv*, 2019.
- [38] T Konstantin Rusch, Michael M Bronstein, and Siddhartha Mishra. A survey on oversmoothing in graph neural networks. *ArXiv*, 2023.
- [39] Franco Scarselli, Marco Gori, Ah Chung Tsoi, Markus Hagenbuchner, and Gabriele Monfardini. The graph neural network model. *IEEE Transactions on Neural Networks*, 2009.

- [40] Guodong Shi, Claudio Altafini, and John S Baras. Dynamics over signed networks. *SIAM Review*, 2019.
- [41] Yunchong Song, Chenghu Zhou, Xinbing Wang, and Zhouhan Lin. Ordered gnn: Ordering message passing to deal with heterophily and over-smoothing. *arXiv preprint arXiv:2302.01524*, 2023.
- [42] Anton Tsitsulin, John Palowitch, Bryan Perozzi, and Emmanuel Müller. Graph clustering with graph neural networks. *Journal of Machine Learning Research*, 2023.
- [43] Petar Veličković, Guillem Cucurull, Arantxa Casanova, Adriana Romero, Pietro Liò, and Yoshua Bengio. Graph attention networks. In *ICLR*, 2018.
- [44] Yifei Wang, Yisen Wang, Jiansheng Yang, and Zhouchen Lin. Dissecting the diffusion process in linear graph convolutional networks. In *NeurIPS*, 2021.
- [45] Yuelin Wang, Kai Yi, Xinliang Liu, Yu Guang Wang, and Shi Jin. ACMP: Allen-cahn message passing with attractive and repulsive forces for graph neural networks. In *ICLR*, 2022.
- [46] Felix Wu, Amauri Souza, Tianyi Zhang, Christopher Fifty, Tao Yu, and Kilian Weinberger. Simplifying graph convolutional networks. In *ICML*, 2019.
- [47] Xinyi Wu, Amir Ajorlou, Zihui Wu, and Ali Jadbabaie. Demystifying oversmoothing in attention-based graph neural networks. In *NeurIPS*, 2023.
- [48] Xinyi Wu, Zhengdao Chen, William Wang, and Ali Jadbabaie. A non-asymptotic analysis of oversmoothing in graph neural networks. In *ICLR*, 2023.
- [49] Keyulu Xu, Chengtao Li, Yonglong Tian, Tomohiro Sonobe, Ken-ichi Kawarabayashi, and Stefanie Jegelka. Representation learning on graphs with jumping knowledge networks. In *ICLR*, 2018.
- [50] Keyulu Xu, Weihua Hu, Jure Leskovec, and Stefanie Jegelka. How powerful are graph neural networks? In *ICLR*, 2019.
- [51] Yujun Yan, Milad Hashemi, Kevin Swersky, Yaoqing Yang, and Danai Koutra. Two sides of the same coin: Heterophily and oversmoothing in graph convolutional neural networks. In *ICDM*, 2022.
- [52] Lingxiao Zhao and Leman Akoglu. PairNorm: Tackling oversmoothing in gnns. *ArXiv*, 2019.
- [53] Lingxiao Zhao and Leman Akoglu. Pairnorm: Tackling oversmoothing in gnns. In *ICLR*, 2020.
- [54] Kaixiong Zhou, Xiao Huang, Daochen Zha, Rui Chen, Li Li, Soo-Hyun Choi, and Xia Hu. Dirichlet energy constrained learning for deep graph neural networks. *Advances in Neural Information Processing Systems*, 34:21834–21846, 2021.

# Appendix

## Contents

<b>A</b>	<b>Related Work</b>	<b>16</b>
<b>B</b>	<b>More Discussion on GNNs</b>	<b>16</b>
B.1	Message-passing Graph Neural Networks (MP-GNNs)	16
B.2	GCN	17
B.3	SGC	17
<b>C</b>	<b>More Background about Signed Graph</b>	<b>17</b>
C.1	Signed Graph Propagation	17
C.2	Definition of negative graph	18
C.3	Positive / Negative Interaction	18
C.4	Deterministic Networks	18
<b>D</b>	<b>Analysis of Previous methods via Signed Graph</b>	<b>19</b>
D.1	Discussion of Normalization	19
D.2	Discussion of Residual Connection	21
D.3	Discussion of DropMessage	22
<b>E</b>	<b>Proof of Theorem 4.1</b>	<b>22</b>
<b>F</b>	<b>Proof of Theorem 4.3</b>	<b>23</b>
<b>G</b>	<b>The relationship of oversmoothing and Theorem 4.1 and Theorem 4.3</b>	<b>24</b>
<b>H</b>	<b>Extension of Structural Balance</b>	<b>25</b>
<b>I</b>	<b>Discussion about <math>STD</math></b>	<b>26</b>
I.1	Definition of CSBM	26
I.2	Measure of $STD$	26
I.3	Proof of Proposition 4.6	26
I.4	More observations of $STD$	27
<b>J</b>	<b>Proof of Proposition 4.6 and 4.7</b>	<b>27</b>
<b>K</b>	<b>More Discussion on Structural Balance Propagation</b>	<b>28</b>
<b>L</b>	<b>Time Complexity Analysis and the Modified SBP</b>	<b>28</b>
<b>M</b>	<b>Details of Experiments</b>	<b>29</b>
M.1	Details of the Dataset	29
M.2	Experiments Setup	30

M.3 Results Analysis . . . . .	30
M.3.1 CSBM results . . . . .	30
M.3.2 GCN Results . . . . .	30
M.3.3 Repulsion ablation on heterophilic datasets . . . . .	31
M.3.4 Performance of SBP on more benchmarks . . . . .	32
M.3.5 Combine SBP to other methods . . . . .	32
M.3.6 Performance of SBP on Large-scale graphs . . . . .	32
M.3.7 Further Optimization based on SBP . . . . .	33

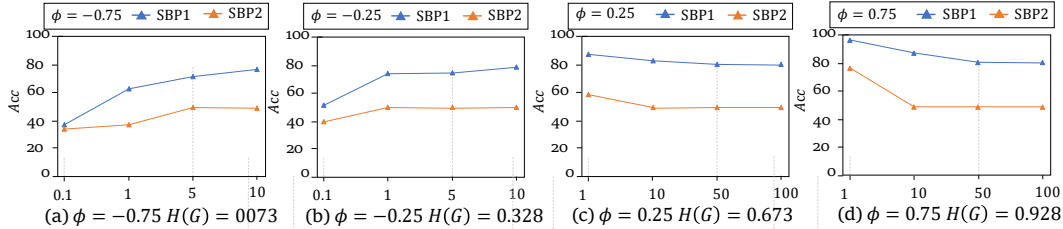


Figure 5: Figure (a)-(d) shows the effect of negative graph weight  $\beta$  by SBP on CSBM. In all cases,  $\lambda = 0.5$  and  $\alpha = 1$ . The X-axis is the  $\beta$  and the Y-axis is the test accuracy.  $\phi$  is the hyperparameter to control the level of homophily and  $H(G)$  measure the homophily level. SBP1 indicates Label-SBP and SBP2 indicates Feature-SBP.

## A Related Work

**Theory of Oversmoothing** The concept of oversmoothing was initially introduced by [26]: when the number of layers becomes large, the representations of different nodes tend to converge to a common value after excessively exchanging messages with neighboring nodes. [34, 47] rigorously show that the convergence of node representations to a common value happens at an exponential rate as the number of layers increases to infinity, for GCNs and attention-based GNNs, respectively. [48] theoretically proves that oversmoothing can start to happen even in shallow depth under certain random graph settings. [54] proposed an appropriate residual connection according to the lower limit of Dirichlet energy and connected to previous methods qualitatively.

**Signed Graph Inspired Methods** In the heterophilic graphs, various methods are inspired by the signed graph propagation [10, 41, 42, 45, 51]. In particular, Wang et al. [45], Yan et al. [51] utilize the idea that the negative edges denote connections between nodes that are "not similar to each other" to create repulsion between them during message-passing. [10] extend the coefficients of the output of different layers in the final aggregation to be learnable and find that the odd layer coefficients tends to be negative for heterophilic graphs, suggesting that learning naturally finds signed-graph message-passing. However, [29] show that under some specific random graph settings, the oversmoothing will even happen under signed graph propagation. Nevertheless, we extend the theory to generic graphs and prove that in the ideal state—structural balance, signed edges can indeed serve as a remedy to effectively combat oversmoothing.

**Structural Balance** Structural balance theory has gained significant attention in recent years [13, 28, 45, 51]. Inspired by the structural balance theory, [13] characterizes the balanced path intuitively to learn both balanced and unbalanced representations on each layer. [28] predicts the signed adjacency matrix by an off-the-shelf neural network classifier to generate pseudo labels with the low-rank assumption. [40] introduces the definition of the Laplacian for signed graphs and develops a comprehensive mathematical theory. In this paper, we rigorously show that structural balance is the theoretical solution to alleviate oversmoothing and propose practical methods based on the property without any additional learnable parameters.

## B More Discussion on GNNs

### B.1 Message-passing Graph Neural Networks (MP-GNNs)

Let  $\mathcal{G} = (A, X)$  denote a graph with  $n$  nodes and  $m$  edges, where  $A \in \{0, 1\}^{n \times n}$  is the adjacency matrix, and  $X \in \mathbb{R}^{n \times d}$  is the node feature matrix with a node feature dimension of  $d$ . Usually, we will transform the concrete adjacency matrix  $A$  to the normalized adjacency matrix  $\hat{A}$  by the degree matrix. Define  $D = \text{diag}(d_1, d_2, \dots, d_n)$  where  $d_i$  is the degree of the node  $i$ . Then the normalized adjacency matrix  $\hat{A} = D^{-\frac{1}{2}}AD^{-\frac{1}{2}}$ . Moreover, many theoretical works simplified the normalized adjacency matrix to be  $D^{-1}A$  or  $AD^{-1}$  as the row-normalized or column-normalized stochastic matrix where the sum of every row (column) is 1 and every entry is non-negative. In this paper, we use  $\hat{A} = D^{-\frac{1}{2}}AD^{-\frac{1}{2}}$ .



Different GNNs typically share a common propagation mechanism, where node features are aggregated and transformed along the network’s topology to a certain depth. The  $k$ -th layer propagation can be formalized as

$$H_{(k)} = \mathbf{PROPAGATE}(X; \mathcal{G}; k) = \left\langle \mathbf{Trans} \left( \mathbf{Agg} \{ \mathcal{G}; H_{(k-1)} \} \right) \right\rangle_k, \quad (9)$$

with  $H_{(0)} = X$  and  $H_{(k)}$  is the output after the  $k$ -layer propagation. The notation  $\langle \cdot \rangle_k$  generally varies from GNN models and denotes the generalized combination operation following  $k$  convolutions.  $\mathbf{Agg} \{ \mathcal{G}; H_{(k-1)} \}$  refers to aggregating the  $(k-1)$ -layer output  $\mathbf{H}^{(k-1)}$  along graph  $\mathcal{G}$ . Meanwhile,  $\mathbf{Trans}(\cdot)$  is the corresponding layer-wise feature transformation which often includes a non-linear activation function (e.g., ReLU) and a layer-specific learnable weight matrix  $W$  for transformation

## B.2 GCN

To deal with non-Euclidean graph data, GCNs are proposed for direct convolution operation over graph, and have drawn interests from various domains. GCN is firstly introduced for a spectral perspective [25], but soon it becomes popular as a general message-passing algorithm in the spatial domain. In the feature transformation stage, GCN adopts a non-linear activation function (e.g., ReLU) and a layer-specific learnable weight matrix  $W$  for transformation. The propagation rule of GCN can be formulated as follow:

$$H_{(k)} = \text{ReLU}((\hat{A}H_{(k-1)})W_{(k)}) \quad (10)$$

## B.3 SGC

SGC [46] simplifies and separates the two stages of GCNs: feature propagation and (non-linear) feature transformation. It finds that utilizing only a simple logistic regression after feature propagation (removing the non-linearities), which makes it a linear GCN, can obtain comparable performance to canonical GCNs. The propagation rule of GCN can be formulated as follow:

$$H_{(k)} = \hat{A}H_{(k-1)}W_{(k)} = \hat{A}^k H_{(0)}W_{(k)} \dots W_{(1)} \quad (11)$$

Moreover, SGC transforms  $W_{(k)} \dots W_{(1)}$  to a general learnable parameter  $W$ , so the formula of SGC can be this:

$$H_{(k)} = \hat{A}^k H_{(0)}W \quad (12)$$

## C More Background about Signed Graph

### C.1 Signed Graph Propagation

Classical GNNs [25, 43, 46, 50] primarily focused on message-passing on unsigned graphs or graphs composed solely of positive edges. For example, if there exists a edge  $\{i, j\}$  or the sign of edge  $\{i, j\}$  is positive, the node  $x_i$  updates its value by:

$$\hat{x}_i = x_i + \alpha(x_j - x_i) = (1 - \alpha)x_i + \alpha x_j, \alpha \in (0, 1). \quad (13)$$

Compared to the unsigned graph, a signed graph extends the edges to either positive or negative. Notably, if the sign of edge  $\{i, j\}$  is negative, the node  $x_i$  update its value using the following expression:

$$\hat{x}_i = x_i - \beta(x_j - x_i) = (1 + \beta)x_i - \beta x_j, \beta \in (0, 1). \quad (14)$$

In words, the positive interaction equation 13 indicates the attraction while the negative interaction equation 14 indicates that the nodes will repel their neighbors.

More generally, when considering all of the neighbors of node  $x_i$ , let  $N_i^+$  denote the positive neighbor set while  $N_i^-$  denote the negative neighbor set, where  $N_i^+ \cup N_i^- = N_i$  and  $N_i^+ \cap N_i^- = \emptyset$ . The representation of  $x_i$  is thus updated by:

$$\hat{x}_i = (1 - \alpha + \beta)x_i + \frac{\alpha}{|N_i^+|} \sum_{j \in N_i^+} x_j - \frac{\beta}{|N_i^-|} \sum_{j \in N_i^-} x_j. \quad (15)$$

In particular, the two parameters  $\alpha$  and  $\beta$  mark the strength of positive and negative edges, respectively. Furthermore, the signed propagation rule equation 15 from a single node can be generalized over the whole graph  $\mathcal{G}$  written in the matrix update form as:

$$\hat{X} = (1 - \alpha + \beta)X + \alpha\hat{A}^+X - \beta\hat{A}^-X, \quad (16)$$

where  $\hat{A}^+$  is the raw normalized version of the positive adjacency matrix  $A^+ \in \{0, 1\}^{n \times n}$  and  $\hat{A}^-$  is that of the negative adjacency matrix  $A^- \in \{0, 1\}^{n \times n}$ .

## C.2 Definition of negative graph

For further proofs of the theorems and propositions in the paper, we give a more simple and detailed definition in this section.

Let  $D_{G^+} = \text{diag}(\text{deg}_1^+, \dots, \text{deg}_n^+)$  and  $D_{G^-} = \text{diag}(\text{deg}_1^-, \dots, \text{deg}_n^-)$  be the degree matrices of the positive subgraph and negative subgraph, respectively. Let  $A_{G^+}$  be the adjacency matrix of the graph  $G^+$  with  $[A_{G^+}]_{ij} = 1$  if  $\{i, j\} \in E^+$  and  $[A_{G^+}]_{ij} = 0$  otherwise. The adjacency matrix  $A_{G^-}$  of the negative subgraph  $G^-$  is defined by  $[A_{G^-}]_{ij} = -1$  for  $\{i, j\} \in E^-$  and  $[A_{G^-}]_{ij} = 0$  for  $\{i, j\} \notin E^-$ .

The Laplacian plays a central role in the algebraic representation of structural properties of graphs. In the presence of negative edges, more than one definition of Laplacian is possible; see [40]. The Laplacian of the positive subgraph  $G^+$  is  $L_{G^+} := D_{G^+} - A_{G^+}$ , while for the negative subgraph  $G^-$  the following two variants can be used:  $L_{G^-}^o := D_{G^-} - A_{G^-}$  and  $L_{G^-}^r := -D_{G^-} - A_{G^-}$ . Consequently, we have the following definitions.

Definition 1. Given the signed graph  $G$ , its opposing Laplacian is defined as

$$L_G^o := L_{G^+} + L_{G^-}^o = D_{G^+} + D_{G^-} - A_{G^+} - A_{G^-}, \quad (17)$$

and its repelling Laplacian is defined as

$$L_G^r = L_{G^+} + L_{G^-}^r = D_{G^+} - D_{G^-} - A_{G^+} - A_{G^-}. \quad (18)$$

## C.3 Positive / Negative Interaction

Time is slotted at  $t = 0, 1, \dots$ . Each node  $i$  holds a state  $x_i(t) \in \Omega$  at time  $t$  and interacts with its neighbors at each time to revise its state. The interaction rule is specified by the sign of the links. Let  $\alpha, \beta \geq 0$ . We first focus on a particular link  $\{i, j\} \in E$  and specify for the moment the dynamics along this link isolating all other interactions.

The DeGroot Rule:

$$x_s(t+1) = x_s(t) + \alpha(x_{-s}(t) - x_s(t)) = (1 - \alpha)x_s(t) + \alpha x_{-s}(t), \quad (19)$$

where  $-s \in \{i, j\} \setminus \{s\}$  with  $\alpha \in (0, 1)$

The Opposing Rule:

$$x_s(t+1) = x_s(t) + \beta(-x_{-s}(t) - x_s(t)) = (1 - \beta)x_s(t) - \beta x_{-s}(t); \quad (20)$$

or The Repelling Rule:

$$x_s(t+1) = x_s(t) - \beta(x_{-s}(t) - x_s(t)) = (1 + \beta)x_s(t) - \beta x_{-s}(t). \quad (21)$$

## C.4 Deterministic Networks

The Repelling Negative Dynamics:

$$\begin{aligned} x_i(t+1) &= x_i(t) + \alpha \sum_{j \in N_i^+} (x_j(t) - x_i(t)) - \beta \sum_{j \in N_i^-} (x_j(t) - x_i(t)) \\ &= (1 - \alpha \text{deg}_i^+ + \beta \text{deg}_i^-) x_i(t) + \alpha \sum_{j \in N_i^+} x_j(t) - \beta \sum_{j \in N_i^-} x_j(t). \end{aligned} \quad (22)$$

Denote  $\mathbf{x}(t) = (x_1(t) \dots x_n(t))^T$ . We can now rewrite 22 in the compact form

$$\mathbf{x}(t+1) = M_G \mathbf{x}(t) = (I - \alpha L_{G^+} - \beta L_{G^-}^r) \mathbf{x}(t). \quad (23)$$

Here,

$$M_G = I - \alpha L_{G^+} - \beta L_{G^-}^r = I - L_G^{rw}, \quad (24)$$

with  $L_G^{rw} = \alpha L_{G^+} + \beta L_{G^-}^r$  being the repelling weighted Laplacian of  $G$ . From Equation 23,  $M_G \mathbf{1} = \mathbf{1}$  always holds. We present the following result, which by itself is merely a straightforward look into the spectrum of the repelling Laplacian  $L_G^{rw}$ .

Note that our equation 1 is consistent with Equation equation 22, only need to replace the  $\alpha$  and  $\beta$  with  $\frac{\alpha}{deg_i^+}$  and  $\frac{\beta}{deg_i^-}$  respectively.

## D Analysis of Previous methods via Signed Graph

### D.1 Discussion of Normalization

**BatchNorm** BatchNorm centers the node representations  $X$  to zero mean and unit variance and can be written as  $\text{BatchNorm}(x_i) = \frac{1}{\sqrt{\sigma^2 + \epsilon}}(x_i - \frac{1}{n} \sum_{i=1}^n x_i)$ , where  $\epsilon > 0$  and  $\sigma^2$  is the variance of node features. We rewrite BatchNorm in the signed graph propagation form as follows:

$$\hat{X} = \hat{A} X \Gamma_d^{-1} - \frac{\mathbf{1}_n \mathbf{1}_n^T}{n} \hat{A} X \Gamma_d^{-1} = \hat{A} \tilde{X} - \frac{\mathbf{1}_n \mathbf{1}_n^T}{n} \hat{A} \tilde{X}, \quad (25)$$

where  $\Gamma_d = \text{diag}(\sigma_1, \dots, \sigma_d)$  is a diagonal matrix that represents column-wise variance with  $\sigma_i^2 = \frac{1}{n} \sum_{j=1}^n ((\hat{A}X)_{ji} - \mathbf{1}_n^T \hat{A}X/n)^2$ , and  $\tilde{X} = X \Gamma_d^{-1}$  is a normalized version of  $X$ . We can correspond to the positive graph  $A^+$  to  $\hat{A}$  and the negative graph  $A^-$  to  $\frac{\mathbf{1}_n \mathbf{1}_n^T}{n} \hat{A}$  in Eq. equation 25.

**PairNorm** We then introduce another method called PairNorm where the only difference between it and BatchNorm is that PairNorm scales all the entries in  $X$  using the same number rather than scaling each column by its own variance. The formulation of PairNorm can be rewritten as follows:

$$\hat{X} = \frac{1}{\Gamma} \hat{A} X - \frac{1}{\Gamma} \frac{\mathbf{1}_n \mathbf{1}_n^T}{n} \hat{A} X = \frac{1}{\Gamma} (\hat{A} X - \frac{\mathbf{1}_n \mathbf{1}_n^T}{n} \hat{A} X), \quad (26)$$

where  $\Gamma = \|(\hat{A} - \frac{\mathbf{1}_n \mathbf{1}_n^T}{n})X\|_F / \sqrt{n}$ . We observe that PairNorm shares the same positive and negative graphs (up to scale) as BatchNorm. Another normalization technique, ContraNorm, turns out to extend the negative graph to an adaptive one based on node feature similarities.

**ContraNorm** ContraNorm is inspired by the uniformity loss from contrastive learning, aiming to alleviate dimensional feature collapse. For simplicity, we consider the spectral version of ContraNorm that takes the following form:

$$\hat{X} = (1 + \alpha) \hat{A} X - \alpha / \tau (X X^T) \hat{A} X, \quad (27)$$

where  $\alpha \in (0, 1)$  and  $\tau > 0$  are hyperparameters. We can see that  $\hat{A}$  is again the positive graph and  $(X X^T) \hat{A}$  is the negative graph in the corresponding signed graph propagation.

**Proposition D.1** Consider the update:

$$\hat{X} = A X - \frac{\mathbf{1}_n \mathbf{1}_n^T}{n} A X, \quad (28)$$

where  $A \in \{0, 1\}^{n \times n}$  is the adjacency matrix. Define the overall signed graph adjacency matrix  $A_s$  as  $A - \frac{\mathbf{1}_n \mathbf{1}_n^T}{n} A$ . Then we have that the signed graph is (weakly) structurally balanced only if the original graph can be divided into several isolated complete subgraphs.

**Proof.** Assume that there is no isolated node and no node has edges with all the other nodes.  $(A_s)_{i,j} = (A)_{i,j} - \frac{deg_j}{n}$ . If  $(A)_{i,j} = 1$ , then we have  $(A_s)_{i,j} > 0$ . If  $(A)_{i,j} = 0$ , then we have  $(A_s)_{i,j} < 0$ .

If the nodes can be divided into several isolated complete subgraphs, then the nodes set  $V = V_1 \cup V_2 \dots V_m$ , where  $|V_i| > 1$ ,  $m$  is the number of the isolated complete subgraphs. So only the nodes within the same set have edges, thus relative entries of  $A_s > 0$ , while nodes from different sets do not, thus relative entries of  $A_s < 0$ .

On the other hand, if  $A_s$  is (weakly) structurally balanced, then the nodes set can be expressed as  $V = V_1 \cup V_2 \dots V_k$ , where  $|V_i| > 1$ ,  $k$  is the number of the separated parties in the signed graph. The entry of  $A_s$  in the same parties is positive, while between different parties is negative. According to  $(A_s)_{i,j} = (A)_{i,j} - \frac{deg_j}{n}$ , we know that nodes in the same parties are connected in the original graph while not connected in the original graph between different parties. So the graph can be divided into several isolated complete subgraphs.

Overall, the signed graph is (weakly) structurally balanced only if the original graph can be divided into several isolated complete subgraphs, the proof is over.

The Proposition shows that in order for the structural balance property to hold for the signed graph of normalization, the graph needs to satisfy an unrealistic condition where the edges strictly cluster the nodes.

**Discussion of ContraNorm** Consider the update:

$$\hat{X} = AX - \frac{XX^T}{n}AX, \quad (29)$$

Define the overall signed graph adjacency matrix  $A_s = A - \frac{XX^T}{n}A$  where  $(A_s)_{i,j} = (A)_{i,j} - \frac{1}{n} \sum_{k=1}^n x_i x_k^T (A)_{k,j}$ .

Assume that the nodes feature is normalized every update, that is  $\|x_i\|_2 = 1$  for every  $i$ .

If  $(A)_{i,j} = 1$ , then we have that

$$\begin{aligned} (A_s)_{i,j} &= (A)_{i,j} - \frac{1}{n} \sum_{k=1}^n x_i x_k^T (A)_{k,j} \\ &= 1 - \frac{1}{n} \sum_{k=1}^n x_i x_k^T (A)_{k,j} \\ &> 1 - \frac{1}{n} \sum_{k=1}^n (A)_{k,j} \\ &= 1 - \frac{d_j}{n} > 0. \end{aligned} \quad (30)$$

That means if  $(A)_{i,j} = 1$ , then  $(A_s)_{i,j} > 0$ . However, if  $(A)_{i,j} = 0$ , then we have that

$$\begin{aligned} (A_s)_{i,j} &= (A)_{i,j} - \frac{1}{n} \sum_{k=1}^n x_i x_k^T (A)_{k,j} \\ &= -\frac{1}{n} \sum_{k=1}^n x_i x_k^T (A)_{k,j} \\ &= -\frac{1}{n} \sum_{k \in N_j} x_i x_k^T. \end{aligned} \quad (31)$$

Intuitively, if  $x_i$  has similar features to  $x_j$ 's neighbors, then we have that  $(A_s)_{i,j} < 0$ , which means trying to repel nodes with similar representations. If  $x_i$  has different features to  $x_j$ 's neighbors, then we have that  $(A_s)_{i,j} > 0$ , which means trying to aggregate nodes with original different representations.

If graph  $G$  is a completed graph, then all entries of  $(A_s) > 0$ , however, when all of the nodes coverage to each other,  $\sum_{k=1}^n x_i x_k^T (A)_{k,j} = \sum_{k=1}^n x_i x_k^T$  will also become bigger.

## D.2 Discussion of Residual Connection

The standard residual connection [8, 44] directly combines the previous and the current layer features together. It can be formulated as:

$$\hat{X} = (1 - \alpha)X + \alpha\hat{A}X = X + \alpha\hat{A}X - \alpha IX. \quad (32)$$

For residual connections, the positive adjacency matrix is  $\hat{A}$  and the negative adjacency matrix  $I$  in the corresponding signed graph propagation.

**APPNP** We reformulate the method APPNP [19] as the signed propagation form of the initial node feature. Another propagation process is APPNP [19] which can be viewed as a layer-wise graph convolution with a residual connection to the initial transformed feature matrix  $X^{(0)}$ , expressed as:

$$\hat{X}^{(k+1)} = (1 - \alpha)X^{(0)} + \alpha\hat{A}X^{(k)}. \quad (33)$$

**Theorem D.2** With  $\hat{A}^+ = \sum_{i=0}^{k+1} \alpha^i \hat{A}^i$  and  $\hat{A}^- = \alpha \sum_{j=0}^k \alpha^j \hat{A}^j$ , the propagation process of APPNP following the signed graph propagation.

**Proof.** Easily prove with mathematical induction.

In addition to combining with the last and initial layer features, the last type integrates several intermediate layer features. The established representations are JKNET [49] and DAGNN [30].

**JKNET** JKNET is a deep graph neural network which exploits information from neighborhoods of differing locality. JKNET selectively combines aggregations from different layers with Concatenation/Max-pooling/Attention at the output, i.e., the representations "jump" to the last layer. Using attention mechanism for combination at the last layer, the  $k + 1$ -layer propagation result of JKNET can be written as:

$$\begin{aligned} X^{(k+1)} &= \alpha_0 X^{(0)} + \alpha_1 X^{(1)} + \dots + \alpha_k X^{(k)} \\ &= \sum_{i=0}^k \alpha_i \hat{A}^i X^{(0)}, \end{aligned} \quad (34)$$

where  $\alpha_0, \alpha_1, \dots, \alpha_k$  are the learnable fusion weights with  $\sum_{i=0}^k \alpha_i = 1$ .

**DAGNN** Deep Adaptive Graph Neural Networks (DAGNN) [30] tries to adaptively add all the features from the previous layer to the current layer features with the additional learnable coefficients. After decoupling representation transformation and propagation, the propagation mechanism of DAGNN is similar to that of JKNET.

$$X^{(k+1)} = \sum_{i=0}^k \alpha_i \hat{A}^i H^{(0)}, \quad H^{(0)} = f_\theta(X^{(0)}) \quad (35)$$

$H^{(0)} = f_\theta(X^{(0)})$  is the non-linear feature transformation using an MLP network, which is conducted before the propagation process and  $\alpha_0, \alpha_1, \dots, \alpha_k$  are the learnable fusion weights with  $\sum_{i=0}^k \alpha_i = 1$ .

**Theorem D.3** With  $\hat{A}^+ = \sum_{i=0}^{k-1} \alpha^i \hat{A}^i + \hat{A}^k$  and  $\hat{A}^- = \sum_{j=0}^{k-1} \alpha^j \hat{A}^j$ , the propagation process of JKNET and DAGNN following the signed graph propagation.

**Proof.** Easily prove with mathematical induction.

As for more residual inspired methods [9, 16, 17, 31], we select GCNII and wGCN to give a detailed discussion as follows.

- As for GCNII [9], it is an improved version of APPNP with the learnable coefficients  $\alpha_i$  and changes the learnable weight  $W$  to  $(1 - \beta_i)I + \beta_i W$  each layer, so it shares the same positive and negative graph as APPNP.
- As for the wGCN [17], it incorporates trainable channel-wise weighting factors  $\omega$  to learn and mix multiple smoothing and sharpening propagation operators at each layer, same as the init residual combines but change parameters  $\alpha$  to be learnable with a more detailed selection strategy.

### D.3 Discussion of DropMessage

For DropMessage [18], it is a unified way of DropNode, DropEdge and Dropout but with a more flexible mask strategy. We have discussed the DropNode and DropEdge in our paper. DropMessage can be viewed as randomly dropping some dimension of the aggregated node features instead of the whole node or the whole edge. We give the unified positive and negative graph of DropMessage in the term of the signed graph. The propagation of DropMessage can be expressed as  $H^{(k)} = AH^{(k-1)} - M_m$ , where if dropping  $AH_{ij}^{(k-1)}$ , then  $M_{ij} = AH_{ij}^{(k-1)}$  else  $M_{ij} = 0$ .

## E Proof of Theorem 4.1

Now consider the combined theorem.

**Theorem E.1** *Suppose that the positive edges are connected. Then along Equation 22 for any  $0 < \alpha < 1/\max_{i \in V} \deg_i^+$ , there exists a critical value  $\beta_* \geq 0$  for  $\beta$  such that*

- (i) *if  $\beta < \beta_*$ , then we have  $\lim_{t \rightarrow \infty} x_i(t) = \sum_{j=1}^n x_j(0)/n$  for all initial values  $x(0)$ ;*
- (ii) *if  $\beta > \beta_*$ , then  $\lim_{t \rightarrow \infty} \|x(t)\| = \infty$  for almost all initial values w.r.t. Lebesgue measure.*

**Proof.** we change the signed graph update to the equivalent version of  $x_i(t)$  read as:

$$x_i(t+1) = x_i(t) + \alpha \sum_{j \in N_i^+} (x_j(t) - x_i(t)) - \beta \sum_{j \in N_i^-} (x_j(t) - x_i(t)).$$

This can be expressed as:

$$x(t+1) = (1 - \alpha \deg^+ + \beta \deg^-)x_i(t) + \alpha \sum_{j \in N^+} x_j(t) - \beta \sum_{j \in N^-} x_j(t). \quad (36)$$

Algorithm 36 can be written as:

$$x(t+1) = M_G x(t) = (I - \alpha L_G^+ - \beta L_G^-)x(t). \quad (37)$$

Here,  $M_G = I - \alpha L_G^+ - \beta L_G^-$ , with  $L_G^+ = \alpha L_G^+ + \beta L_G^-$  being the repelling weighted Laplacian of  $G$ , defined in Sec.C.2. From Eq.equation 37,  $M_G \mathbf{1} = \mathbf{1}$  always holds. We present the following result, which by itself is merely a straightforward look into the spectrum of the repelling Laplacian  $L_G^-$ .

So theorem E.1 can be changed to the following version:

Suppose  $G^+$  is connected. Then along Eq.equation 37 for any  $0 < \alpha < 1/\max_{i \in V} \deg_i^+$ , there exists a critical value  $\beta > 0$  for  $\beta$  such that:

- (i) *if  $\beta < \beta_*$ , then average consensus is reached in the sense that  $\lim_{t \rightarrow \infty} x_i(t) = \frac{1}{n} \sum_{j=1}^n x_j(0)$  for all initial values  $x(0)$ ;*
- (ii) *if  $\beta > \beta_*$ , then  $\lim_{t \rightarrow \infty} \|x(t)\| = \infty$  for almost all initial values w.r.t. Lebesgue measure.*

**Proof.** Define  $J = 11^T/n$ . Fix  $\alpha \in (0, 1/\max_{i \in V} \deg_i^+)$  and consider  $f(\beta) = \lambda_{\max}(I - \alpha L_G^+ - \beta L_G^- - J)$ , and  $g(\beta) = \lambda_{\min}(I - \alpha L_G^+ - \beta L_G^- - J)$ . The Courant–Fischer Theorem implies that both  $f(\cdot)$  and  $g(\cdot)$  are continuous and nondecreasing functions over  $[0, \infty)$ . The matrix  $J$  always commutes with  $I - \alpha L_G^+ - \beta L_G^-$ , and 1 is the only nonzero eigenvalue of  $J$ . Moreover, the eigenvalue 1 of  $J$  shares a common eigenvector  $\mathbf{1}$  with the eigenvalue 1 of  $I - \alpha L_G^+ - \beta L_G^-$ .

Since  $G^+$  is connected, the second smallest eigenvalue of  $L_{G^+}$  is positive. Since  $0 < \alpha < \frac{1}{\max_{i \in V} \deg_i^+}$ , there holds  $\lambda_{\min}(I - \alpha L_{G^+}) \geq -1$ , again due to the Gershgorin Circle Theorem. Therefore,  $f(0) < 1$ ,  $g(0) \geq -1$ . Noticing  $f(\infty) = \infty > 1$ , there exists  $\beta_* > 0$  satisfying  $f(\beta_*) = 1$ . We can then verify the following facts:

- There hold  $f(\beta) < 1$  and  $g(\beta) > -1$  if  $\beta < \beta_*$ . In this case, along Eq. equation 37  $\lim_{t \rightarrow \infty} (I - J)x(t) = 0$ , which in turn implies that  $x(t)$  converges to the eigenspace corresponding to the eigenvalue 1 of  $M_G$ . This leads to the average consensus statement in (i).
- There holds  $f(\beta) \geq 1$  if  $\beta > \beta_*$ . In this case, along Eq. equation 37  $x(t)$  diverges as long as the initial value  $x(0)$  has a nonzero projection onto the eigenspace corresponding to  $\lambda_{\max}(M_G)$  of  $M_G$ . This leads to the almost everywhere divergence statement in (ii).

The proof is now complete.

## F Proof of Theorem 4.3

**Theorem F.1** *let  $A > 0$  be a constant and define  $\mathcal{F}(z)_c$  by  $\mathcal{F}(z)_c = -c, z < -c, \mathcal{F}(z)_c = z, z \in [-c, c]$ , and  $\mathcal{F}(z)_c = c, z > c$ . Define the function  $\theta : E \rightarrow \mathbb{R}$  so that  $\theta(\{i, j\}) = \alpha$  if  $\{i, j\} \in E^+$  and  $\theta(\{i, j\}) = -\beta$  if  $\{i, j\} \in E^-$ . Assume that node  $i$  interacts with node  $j$  at time  $t$  and consider the following node interaction under the signed propagation rules:*

$$x_s(t+1) = \mathcal{F}(z)_c((1-\theta)x_s(t) + \theta x_{-s}(t)), \quad s \in \{i, j\}. \quad (38)$$

*let  $\alpha \in (0, 1/2)$ . Assume that  $G$  is a structurally balanced complete graph under the partition  $V = V_1 \cup V_2$ . When  $\beta$  is sufficiently large, for almost all initial values  $x(0)$  w.r.t. Lebesgue measure, there exists a binary random variable  $l(x(0))$  taking values in  $\{-c, c\}$  such that*

$$\mathbb{P} \left( \lim_{t \rightarrow \infty} x_i(t) = l(x(0)), i \in V_1; \lim_{t \rightarrow \infty} x_i(t) = -l(x(0)), i \in V_2 \right) = 1. \quad (39)$$

**Proof.** The proof is based on the following lemmas.

**Lemma F.2** *Fix  $\alpha \in (0, 1)$  with  $\alpha \neq \frac{1}{2}$ . For the dynamics 38 with the random pair selection process, there exists  $\beta^*(\alpha) > 0$  such that*

$$\mathbb{P} \left( \limsup_{t \rightarrow \infty} \max_{i, j \in V} |x_i(t) - x_j(t)| = 2A \right) = 1$$

*for almost all initial beliefs if  $\beta > \beta^*$ .*

**Lemma F.3** *Fix  $\alpha \in (1/2, 1)$  and  $\beta \geq 2/(2\alpha - 1)$ . Consider the dynamics 38 with the random pair selection process. Let  $G$  be the complete graph with  $\kappa(G^+) \geq 2$ . Suppose for time  $t$  there are  $i_1, j_1 \in V$  with  $x_{i_1}(t) = -c$  and  $x_{j_1}(t) = c$ . Then for any  $\epsilon \in [0, (2\alpha - 1)c/2\alpha]$  and any  $i_* \in V$ , the following statements hold:*

- There exist an integer  $Z(\epsilon)$  and a sequence of node pair realizations,  $G_{t+s}(\omega)$ , for  $s = 0, 1, \dots, Z - 1$ , under which  $x_{i_*}(t + Z)(\omega) \leq -A + \epsilon$ .*
- There exist an integer  $Z(\epsilon)$  and a sequence of node pair realizations,  $G_{t+s}(\omega)$ , for  $s = 0, 1, \dots, Z - 1$ , under which  $x_{i_*}(t + Z)(\omega) \geq A - \epsilon$ .*

**Proof.** From our standing assumption, the negative graph  $G^-$  contains at least one edge. Let  $k_*, m_* \in V$  share a negative link. We assume the two nodes  $i_1, j_1 \in V$  labeled in the lemma are different from  $k_*, m_*$ , for ease of presentation. We can then analyze all possible sign patterns among the four nodes  $i_1, j_1, k_*, m_*$ . We present here just the analysis for the case with

$$\{i_1, k_*\} \in E^+, \{i_1, m_*\} \in E^+, \{j_1, k_*\} \in E^+, \{j_1, m_*\} \in E^+.$$

The other cases are indeed simpler and can be studied via similar techniques.

Without loss of generality we let  $x_{m_*}(t) \geq x_{k_*}(t)$ . First of all we select  $G_t = \{i_1, k_*\}$  and  $G_{t+1} = \{j_1, m_*\}$ . It is then straightforward to verify that

$$x_{m_*}(t+2) \geq x_{k_*}(t+2) + 2\alpha c.$$

By selecting  $G_{t+2} = \{m_*, k_*\}$  we know from  $\beta \geq \frac{2}{(2\alpha-1)} > \frac{1}{\alpha}$  that

$$x_{k_*}(t+3) = -c, \quad x_{m_*}(t+3) = c.$$

There will be two cases:

- (a) Let  $i_* \in \{m_*, k_*\}$ . Noting that  $\kappa(G^+) \geq 2$ , there will be a path connecting to  $k_*$  from  $i_*$  without passing through  $m_*$  in  $G^+$ . It is then obvious that we can select a finite number  $Z_1$  of links which alternate between  $\{m_*, k_*\}$  and the edges over that path so that  $x_{i_*}(t+3+Z_1) \geq -c + \epsilon$ . Here  $Z_1$  depends only on  $\alpha$  and  $n$ .
- (b) Let  $i_* \in \{m_*, k_*\}$ . We only need to show that we can select pair realizations so that  $x_{m_*}$  can get close to  $-c$ , and  $x_{k_*}$  gets close to  $c$  after  $t + 3$ . Since  $G^+$  is connected, either  $m_*$  or  $k_*$  has at least one positive neighbor. For the moment assume  $m'$  is a positive neighbor of  $m_*$  and  $k'$  is a positive neighbor of  $k_*$  with  $m' \neq k'$ . Then from part (a) we can select  $Z_2$  node pairs so that

$$x_{m_*}(t+3+Z_2) \leq -c + \epsilon, \quad x_{k_*}(t+3+Z_2) \geq c - \epsilon.$$

Thus, selecting the negative edge  $\{m_*, k_*\}$  for  $t+5+Z_2$  implies  $x_{m_*}(t+6+Z_2) = c$  for  $\beta \geq \frac{2}{(2\alpha-1)}$ . The case with  $m' = k'$  can be dealt with by a similar treatment, leading to the same conclusion.

This concludes the proof of the lemma.

In view of Lemmas F.2 and F.3, the desired theorem is a consequence of the second Borel–Cantelli Lemma.

## G The relationship of oversmoothing and Theorem 4.1 and Theorem 4.3

**Discussion with other training methods** While [35] questions the existence of oversmoothing in trained GNNs, their observations are primarily based on specific experimental settings that may not fully capture the oversmoothing challenge present in the literature. Specifically, the empirical observations in [35] are based on 10-layer GCNs, which, while useful for their argument, may not represent the behavior of deeper networks or other GNN architectures. Moreover, Figure 2 in [35] is based on a normalized metric, which might not be the most appropriate. To see this point, suppose one wants to classify two points. In one case, we have 0.01 vs -0.01 and in the other case, we have 100 vs -100. While the normalized distance considered in [35] would be the same for these two cases, the latter case has a much larger margin, and it would be thus much easier to learn a classifier. On the other hand, [11] suggests that the trainability of deep GNNs is more of a problem than over-smoothing. However, over-smoothing naturally presents challenges for training deep GNNs, as when oversmoothing happens, gradients vanish across different nodes. Besides, [11] compares 3 models GCN, ResGCN and GCNII, proving that GCNII is the best backbone. We have adapted our SBP to GCNII in Table 13 and the results showed that our SBP outperforms GCNII on average, especially in the middle layers.

**Measure on oversmoothing** There exist a variety of different approaches to quantify oversmoothing in deep GNNs, here we choose the measure based on the Dirichlet energy on graphs [38, 47].

$$\epsilon(X(t)) = \frac{1}{v} \sum_{i \in V} \sum_{j \in N_i} \|x_i(t) - x_j(t)\|_2^2, \quad (40)$$

where  $v$  is the number of the nodes,  $x_i(t)$  is the node feature of node  $i$  at time  $t$ .  $N_i$  represents the neighbor set of node  $i$ , In the signed graph, it including nodes connected to  $i$  by both positive and negative edges. Oversmoothing means that when the layers are infinity, all of the node features will converge, that is to say  $\lim_{t \rightarrow \infty} \epsilon(X(t)) \rightarrow 0$ .

In Theorem 4.1, there are 2 cases:

- if  $\beta < \beta_*$ , then we have  $\lim_{t \rightarrow \infty} x_i(t) = \sum_{j=1}^n x_j(0)/n$  for all initial values  $x(0)$
- if  $\beta > \beta_*$ , then  $\lim_{t \rightarrow \infty} \|x(t)\| = \infty$  for almost all initial values w.r.t. Lebesgue measure.

In the first case, all the node features will coverage to the mean of them and therefore  $\lim_{t \rightarrow \infty} \epsilon(X(t)) \rightarrow 0$ , then oversmoothing happens. In the second case, the node features will diverge to infinity and thus  $\lim_{t \rightarrow \infty} \epsilon(X(t)) \rightarrow 0$  or  $\infty$  which is also not what we want.

Theorem 4.1 demonstrated that both insufficient repulsion and excessive repulsion caused by the negative graph can hinder performance in signed graph propagation. From this, we conclude



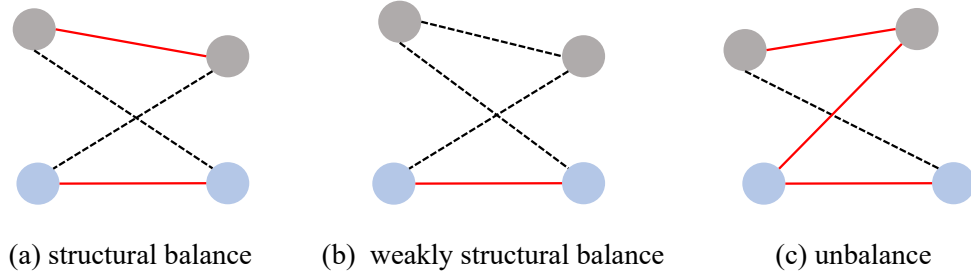


Figure 6: Examples of structural balanced (left), weakly structural balanced (middle), and unbalanced signed graphs (right). Here red lines represent positive edges; black dashed lines represent negative edges; gray and blue circles represent nodes from different labels

that relying solely on the negative signs is insufficient to alleviate oversmoothing. Therefore, we propose the provable solution: a structurally balanced graph to efficiently alleviate oversmoothing in Theorem 4.3. Specifically, we have the following conclusion from the structurally balanced graph in Theorem 4.3:

$$\mathbb{P} \left( \lim_{t \rightarrow \infty} x_i(t) = l(x(0)), i \in V_1; \lim_{t \rightarrow \infty} x_i(t) = -l(x(0)), i \in V_2 \right) = 1. \quad (41)$$

Then we have:

$$\lim_{t \rightarrow \infty} \epsilon(X(t)) = \lim_{t \rightarrow \infty} \frac{1}{v} \sum_{i \in V} \sum_{j \in N_i} \|x_i(t) - x_j(t)\|_2^2 \quad (42)$$

$$= \lim_{t \rightarrow \infty} \frac{1}{v} \sum_{i \in V_1} \sum_{j \in N_i} \|x_i(t) - x_j(t)\|_2^2 + \frac{1}{v} \sum_{i \in V_2} \sum_{j \in N_i} \|x_i(t) - x_j(t)\|_2^2 \quad (43)$$

$$= \lim_{t \rightarrow \infty} \frac{1}{v} \sum_{i \in V_1} \sum_{j \in N_i, y_i \neq y_j} \|x_i(t) - x_j(t)\|_2^2 + \frac{1}{v} \sum_{i \in V_2} \sum_{j \in N_i, y_i \neq y_j} \|x_i(t) - x_j(t)\|_2^2 \quad (44)$$

$$= \lim_{t \rightarrow \infty} \frac{1}{v} \sum_{i \in V_1} \frac{v}{2} \times 2c + \frac{1}{v} \sum_{i \in V_2} \frac{v}{2} \times 2c \quad (45)$$

$$= \lim_{t \rightarrow \infty} \frac{1}{v} \left( \frac{v}{2} \times \frac{v}{2} \times 2c + \frac{v}{2} \times \frac{v}{2} \times 2c \right) \quad (46)$$

$$= vc \geq 0 \quad (47)$$

So Theorem 4.3 proves that under certain conditions, structural balance can alleviate oversmoothing even when the layers are infinity.

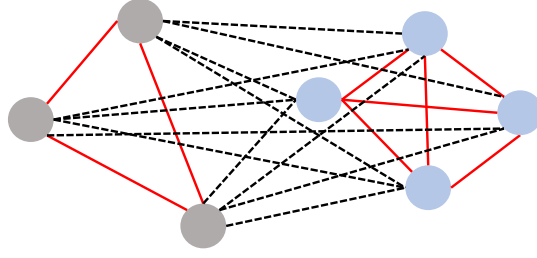
## H Extension of Structural Balance

To clarify the concept of structural balance, weakly structural balance and unbalance signed graph, we give the examples as shown in Figure 6. The notion of structural balance can be weakened in the following definition H.1.

**Definition H.1** A signed graph  $G$  is **weakly structurally balanced** if there is a partition of  $V$  into  $V = V_1 \cup V_2 \cup \dots \cup V_m$ ,  $m \geq 2$  with  $V_1, \dots, V_m$  being nonempty and mutually disjoint, where any edge between different  $V_i$ 's is negative, and any edge within each  $V_i$  is positive.

Then we show that when  $\mathcal{G}$  is a complete graph, weak structural balance also leads to clustering of node states.

**Theorem H.2 ([40], Theorem 10)** Assume that node  $i$  interacts with node  $j$  and  $x_i(t)$  represents the value of node  $i$  at time  $t$ . Let  $\theta = \alpha$  if the edge  $\{i, j\}$  is positive and  $\theta = \beta$  if the edge  $\{i, j\}$  is



structural balance complete graph

Figure 7: Example of structural complete graph. Here red lines represent positive edges; black dashed lines represent negative edges; gray and blue circles represent nodes from different labels

negative. Consider the constrained signed propagation update:

$$x_i(t+1) = \mathcal{F}_c((1-\theta)x_i(t) + \theta x_j(t)). \quad (48)$$

Let  $\alpha \in (0, 1/2)$ . Assume that  $\mathcal{G}$  is a weakly structurally balanced complete graph under the partition  $V = V_1 \cup V_2 \cdots \cup V_m$ . When  $\beta$  is sufficiently large, for almost all initial values  $x(0)$  w.r.t. Lebesgue measure, there exists  $m$  random variable  $l_1(x(0)), l_2(x(0)), \dots, l_m(x(0))$ , each of which taking values in  $\{-c, c\}$  such that

$$\mathbb{P}\left(\lim_{t \rightarrow \infty} x_i(t) = l_j(x(0)), i \in V_j, j = 1, \dots, m\right) = 1. \quad (49)$$

## I Discussion about $SID$

We give the details of CSBM and a more clear formula of  $SID$ ,  $\mathcal{P}$  and  $\mathcal{N}$  as suggested in Tabel 2 in this section.

### I.1 Definition of CSBM

To quantify the structural balance of the mentioned methods, we simplified the graph to 2-CSBM( $N, p, q, \mu_1, \mu_2, \sigma^2$ ) following [48]. It consists of two classes  $\mathcal{C}_1$  and  $\mathcal{C}_2$  of nodes of equal size, in total with  $N$  nodes. For any two nodes in the graph, if they are from the same class, they are connected by an edge independently with probability  $p$ , or if they are from different classes, the probability is  $q$ . For each node  $v \in \mathcal{C}_i, i \in \{1, -1\}$ , the initial feature  $X_v$  is sampled independently from a Gaussian distribution  $\mathcal{N}(\mu_i, \sigma^2)$ , where  $\mu_i = \mathcal{C}_i, \sigma = I$ . In this paper, we assign  $N = 100$  and the feature dimension is 8.

### I.2 Measure of $SID$

$$\mathcal{P} = \frac{1}{|V|} \sum_{v \in V} \text{Number of nodes who have the same label as } v \text{ and the non-positive edge.} \quad (50)$$

$$\mathcal{N} = \frac{1}{|V|} \sum_{v \in V} \text{Number of nodes who have the different label from } v \text{ and the non-negative edge.} \quad (51)$$

$$SB = \frac{1}{2}(\mathcal{P} + \mathcal{N}) \quad (52)$$

### I.3 Proof of Proposition 4.6

**Proposition I.1** For a structural balanced complete graph  $\mathcal{G}$ , we have  $SID(\mathcal{G}) = 0$ .

**Proof** To better understand, we give an example of the structural balance graph as shown in Figure 7. we can see that for a node  $v$ ,  $\mathcal{P}(v) = 0$  and  $\mathcal{N}(v) = 0$  due to the structural balance complete graph assumption. So  $SID(\mathcal{G}) = 0$ .

#### I.4 More observations of $SID$

Apart from Table 2 on CSBM, we further present the Structural Imbalance Degree ( $SID$ ) for Cora across different methods in Table 5. As the performance of these methods is similar in shallow layers (2), we focus on layer 16 to showcase the results.

Table 5:  $SID$  on Cora datasets. We implement all of the methods on SGC under 100 epochs and the accuracy is the result.

	label-SBP	feature-SBP	BatchNorm	ContraNorm	Residual	DropEdge
$\mathcal{P}$	482.1123	482.1123	482.1123	482.1123	482.5137	484.2075
$\mathcal{N}$	0.7408	0.7408	0.7408	0.7408	2221.7305	2221.7305
$SID$	241.4265	241.4265	241.4265	241.4265	1352.1221	1352.9620
Accuracy	$77.43 \pm 1.49$	$77.22 \pm 0.55$	$70.79 \pm 0.00$	$63.35 \pm 0.00$	$40.91 \pm 0.00$	$22.24 \pm 3.04$

We have two key observations: 1) Methods with higher  $SID$  generally lead to worse accuracy, while those with lower  $SID$  tend to produce better accuracy. 2)  $SID$  is a coarse-grained metric; different methods can yield the same  $SID$  values while their performance varies. These observations can also align with the experiments in cSBM in Table 2. The observation may stem from the fact that structural balance is an inherent property of graph structure, which is challenging to measure precisely using a numerical metric like  $SID$ . Proposition 4.6 in the paper proves that when  $SID = 0$ , the graph is structurally balanced. However, for graphs that are not structurally balanced, the properties remain unclear. For future work, we aim to develop a more nuanced metric to quantify the structural balance property of graphs.

## J Proof of Proposition 4.6 and 4.7

**Proposition J.1** Assume that node label classes are balanced  $|Y_1| = |Y_2|$  and denote the ratio of labelled nodes as  $p$ . Then we have that the signed graph adjacency matrix  $A_s = A - A_l$  and  $SID(\mathcal{G}) \leq (1-p)\frac{n}{2}$ , where  $SID$  decreases with a larger labelling ratio  $p$ . In particular, when  $p = 1$  (full supervision), we have  $SID(\mathcal{G}) = 0$ , i.e., a perfectly balanced graph. Under the constrained signed propagation equation 4, the nodes from different classes will converge to distinct constants.

**Proof.** Without loss of generality, assume that the node feature has been normalized which means that  $\|x_i\|_2 = 1$  for every  $i$ . If  $x_i$  and  $x_j$  has the same label, then we have that,  $(A_s)_{i,j} = (A)_{i,j} + 1 > 1$ . If  $x_i$  and  $x_j$  has different labels, then we have that  $(A_s)_{i,j} = (A)_{i,j} - 1 \leq 0$ .

We first prove that  $SID(\mathcal{G}, p) \leq (1-p)\frac{n}{2}$  where  $n$  is the nodes number and  $p$  is the label ratio. We have that

$$\mathcal{P}(v) + \mathcal{N}(v) \leq (1-p)n, \quad (53)$$

because for a single node  $v$  only the remaining  $(1-p)n$  nodes' labels are unknown and therefore their edges may need to change so that

$$\begin{aligned} SID(\mathcal{G}) &= \frac{1}{2n} \sum_{v \in \mathcal{G}} (|\mathcal{P}(v)| + |\mathcal{N}(v)|) \\ &\leq \frac{1}{2n} \sum_{v \in \mathcal{G}} (1-p)n \\ &= (1-p)\frac{n}{2}. \end{aligned} \quad (54)$$

We know that when  $SID(\mathcal{G}) = 0$ , then we have that the nodes  $V$  set can be divided into  $V_1 \cup V_2 \cdots \cup V_L$  where  $L$  is the number of the node classes. There are only positive edges with the node subset and only negative edges between the node subset.

Since  $C = 2$ , the node set can be divided into  $V_1$  and  $V_2$ , the signed graph is structurally balanced. According to Theorem 4.3, we have that the nodes in  $V_1$  will converge to the  $c$  where  $\|c\|_2 = 1$  and the nodes in  $V_2$  will converge to  $-c$ . Thus under Label-SBP propagation, the oversmoothing will only happen within the same label and repel different labels to the boundary.

## K More Discussion on Structural Balance Propagation

The overall update of **Structural Balance Propagation** is as following:

$$X^{(k)} = \text{Layernorm}\{(1 - \lambda)X^{(k-1)} + \lambda(\alpha A^+ X^{(k-1)} - \beta A^- X^{(k-1)})\}, \quad (55)$$

Our methods adopt the normalized adjacency matrix as the positive graph  $A^+ = \hat{A}$ , while use different negative graphs. Although both the positive and negative graphs have hyperparameters, we do not carefully adjust the hyperparameters. Instead, we fix  $\alpha = 1$  and only select the best value for  $\beta$ . You can also change  $\alpha$  and  $\beta$  together to achieve the best performance.

**Label-Induced Negative Graph** The negative graph for Label-SBP is:

$$A^-_{ij} = \begin{cases} 1 & \text{if } i, j \text{ has the different labels,} \\ -1 & \text{if } i, j \text{ has the same labels,} \\ 0 & \text{if } i, j \text{ has the unknown labels.} \end{cases} \quad (56)$$

For practice, we apply softmax to it:

$$\tilde{A}^- = \text{softmax}(A^-). \quad (57)$$

Applying softmax makes the negative graph the row-stochastic which is a non-negative matrix with row sum equal to one. We also tried the normalization method, which is not as good as the softmax. This may be because the softmax method is more aligned with the row-stochastic adjacency, where every element is non-negative.

**Similarity-Induced Negative Graph** The negative graph for Feature-SBP is:

$$A^- = -X^{(0)}X^{(0)T} \quad (58)$$

We also attempted using the last layer node features for the negative graph, but they are not as effective as the initial layer node features. This may be due to oversmoothing as the layers go deeper. For practice, we apply softmax as the Label-SBP to it:

$$\tilde{A}^- = \text{softmax}(-XX^T) \quad (59)$$

## L Time Complexity Analysis and the Modified SBP

**Label-SBP** As shown in equation 4.3, we maintain the positive adjacency matrix  $A^+ = \hat{A}$  and construct the negative adjacency matrix  $A_l$  by assigning 1 when nodes  $i, j$  have different labels, -1 when they share the same label, and 0 when either label is unknown. We then apply softmax to  $A_l$  to normalize the negative adjacency matrix. The overall signed adjacency matrix is  $A_{\text{sign}} = \alpha A^+ - \beta \text{softmax}(A_l)$ , where  $\alpha$  and  $\beta$  are hyperparameters. Given  $n_t$  training nodes and  $d$  edges in the graph, our Label-SBP increases the edge count from  $O(d)$  to  $O(n_t^2)$ , thereby increasing the computational complexity to  $O(n_t^2 d)$ .

**Feature-SBP** When labels are unavailable, we propose Feature-SBP, which uses the similarity matrix of node features to create the negative adjacency matrix. As depicted in equation 4.3, we design the negative adjacency matrix as  $A_f = -X_0 X_0^T$ . We then apply softmax to  $A_f$  to normalize it. The overall matrix follows the same format as Label-SBP:  $A_{\text{sign}} = \alpha A^+ - \beta \text{softmax}(A_f)$ , where  $\alpha$  and  $\beta$  are hyperparameters. The additional computational complexity primarily stems from the negative graph propagation, which involves  $X_0 X_0^T \in \mathbb{R}^{n \times n}$ , increasing the overall complexity to  $O(n^2 d)$ .

We show the computation time of different methods in the Table 6. On average, we improve performance on 8 out of 9 datasets (as shown in Table 15) with less than 0.05s overhead—even faster than three other baselines. We believe this time overhead is acceptable given the benefits it provides.

Table 6: Estimated training time of SBP on Cora dataset. All experiments are run under 2 layers. s is the abbreviation for second. Precompute time is the aggregation time across layers, train time is the update time of the SGC weight  $W$ , total time is the sum of them.

	Label-SBP	Feature-SBP	BatchNorm	ContraNorm	Residual	JKNET	DAGNN	SGC
Precompute time	0.1809s	0.1520s	0.1860s	0.1888s	0.0604s	0.0577s	0.1438s	0.1307s
Train time	0.1071s	0.1060s	0.1076s	0.1038s	0.1368s	0.1446s	0.1348s	0.1034s
Total time	0.2879s	0.2580s	0.2935s	0.2926s	0.1972s	0.2023s	0.2786s	0.2341s
Rank	6	4	8	7	1	2	5	3

**Scalability of SBP on large-scale graph** For large-scale graphs, we introduce a modified version Label-SBP-v2 by only removing edges when pairs of nodes belong to different classes. This approach allows Label-SBP-v2 to eliminate the computational overhead of the negative graph, further enhancing the sparsity of large-scale graphs. For Feature-SBP, as the number of nodes  $n$  increases, the complexity of this matrix operation grows quadratically, i.e.,  $\mathcal{O}(n^2d)$ . To address this, we reorder the matrix multiplication from  $-X_0X_0^T \in \mathbb{R}^{n \times n}$  to  $-X_0^T X_0 \in \mathbb{R}^{d \times d}$ . This preserves the distinctiveness of node representations across the feature dimension, rather than across the node dimension as in the original node-level repulsion. The modified version of Feature-SBP can be expressed as:

$$\text{(Feature-SBP-v2)} \quad X^k = (1 - \lambda)X^{(k-1)} + \lambda(\alpha \hat{A}X^{(K)} - \beta X^{(K)} \text{softmax}(-X_0^T X_0)) \quad (60)$$

This transposed alternative has a linear complexity in the number of samples, i.e.,  $\mathcal{O}(nd^2)$ , significantly reducing the computational burden in cases where  $n \gg d$ .

We compare the compute time SBP with other baselines on ogbn-arxiv dataset over 100 epochs for a fair comparison. Among all the training times of the baselines, our Label-SBP-v2 achieves the 3rd fastest time while Feature-SBP-v2 ranks 5th. Therefore, we recommend using Label-SBP-v2 for large-scale graphs since they typically have a sufficient number of node labels. We believe that although there is a slight time increase, it is acceptable given the benefits.

Table 7: Estimated training time of SBP on ogbn-arxiv dataset. All experiments are run under 2 layers and 100 epochs. s is the abbreviation for second.

	Label-SBP	Feature-SBP	BatchNorm	ContraNorm	DropEdge	SGC
Train time (s)	5.5850	6.1333	5.3872	5.8375	9.5727	5.3097
Rank	3	5	2	4	6	1

## M Details of Experiments

The code for the experiments will be available when our paper is acceptable. We will replace this anonymous link with a non-anonymous GitHub link after the acceptance. We implement all experiments in Python 3.9 with PyTorch Geometric on one NVIDIA Tesla V100 GPU.

### M.1 Details of the Dataset

Table 8: Summary of datasets.  $H(G)$  refers to the edge homophily level: the higher, the more homophilic the dataset is.

Dataset	$H(G)$	Classes	Nodes	Edges
<b>Cora</b>	0.81	7	2,708	5,429
<b>Citeseer</b>	0.74	6	3,327	4,732
<b>PubMed</b>	0.80	3	19,717	44,338
<b>Texas</b>	0.21	5	183	295
<b>Cornell</b>	0.30	5	183	280
<b>Amazon-ratings</b>	0.38	5	24,492	93,050
<b>Wisconsin</b>	0.11	5	251	466
<b>Squirrel</b>	0.22	4	198,493	2,089
<b>Ogbn-Arxiv</b>	0.65	40	16,9343	1,166,243

We consider two types of datasets: Homophilic and Heterophilic. They are differentiated by the *homophily level* of a graph.

$$\mathcal{H} = \frac{1}{|V|} \sum_{v \in V} \frac{\text{Number of } v\text{'s neighbors who have the same label as } v}{\text{Number of } v\text{'s neighbors}}.$$

The low homophily level means that the dataset is more heterophilic when most of the neighbors are not in the same class, and the high homophily level indicates that the dataset is close to homophilic when similar nodes tend to be connected. In the experiments, we use four homophilic datasets, including Cora, CiteSeer, PubMed, and Ogbn-Arxiv, and four heterophilic datasets, including Texas, Wisconsin, Cornell, Squirrel, and Amazon-rating [36]). The datasets we used covers various homophily levels.

## M.2 Experiments Setup

For the SGC backbone, we follow the [44] setting where we run 10 runs for the fixed seed 42 and calculate the mean and the standard deviation. Furthermore, we fix the learning rate and weight decay in the same dataset and run 100 epochs for every dataset. For the GCN backbone, we follow the [22] settings where we run 5 runs from the seed  $\{0, 1, 2, 3, 4\}$  and calculate the mean and the standard deviation. We fix the hidden dimension to 32 and dropout rate to 0.6. Furthermore, we fix the learning rate to be 0.005 and weight decay to be  $5e - 4$  and run 200 epochs for every dataset. We use the default splits in torch\_geometric. We use Tesla-V100-SXM2-32GB in all experiments.

## M.3 Results Analysis

### M.3.1 CSBM results

The comparative results of Label-SBP and Feature-SBP against SGC are presented in Table 9. As the number of layers increases, SGC’s node features suffer from oversmoothing, causing the two classes to converge and accuracy to drop by nearly 30 points from its peak at 2 layers, down to 45%. Conversely, after 300 layers, SBP maintains strong performance, with node features of different classes repelling each other. This effect limits oversmoothing to within-class interactions, and improves performance from 85 to 91 in Label-SBP and from 48 to 82 in Feature-SBP, further substantiating our approach to mitigating oversmoothing.

We visualize the node features learned by Label-SBP in Figure 9. We can see that from layer 0 to layer 200, the node features from different labels repel each other and aggregate the node features from the same labels. And we also visualize the adjacency matrix of Label-SBP and Feature-SBP in Figure 10 and Figure 11 respectively, further verifying the effectiveness of our theorem and insights.

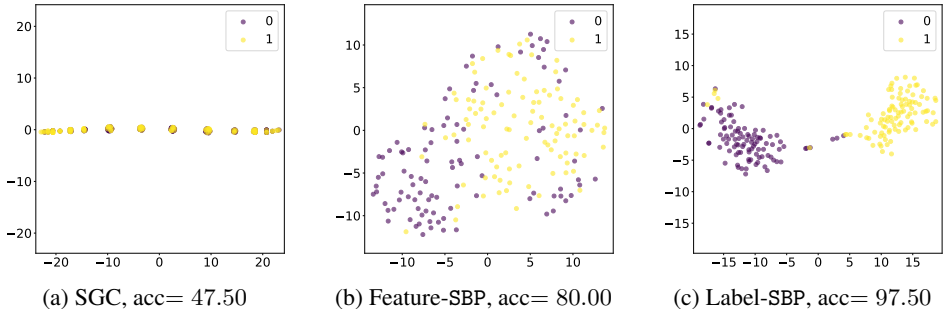


Figure 8: The t-SNE visualization of the node features and the classification accuracy from 2-CSBM and Layer= 300. Left is the result of the vallina SGC, and the middle and right are the results of SBP.

### M.3.2 GCN Results

The results for GCN are detailed in Table 10, respectively. Overall, SBP consistently outperforms all previous methods, especially in deeper layers. Beyond 16 layers in GCN, SBP maintains superior performance, affirming the effectiveness of our approach. Notably, SBP exceeds the best results of

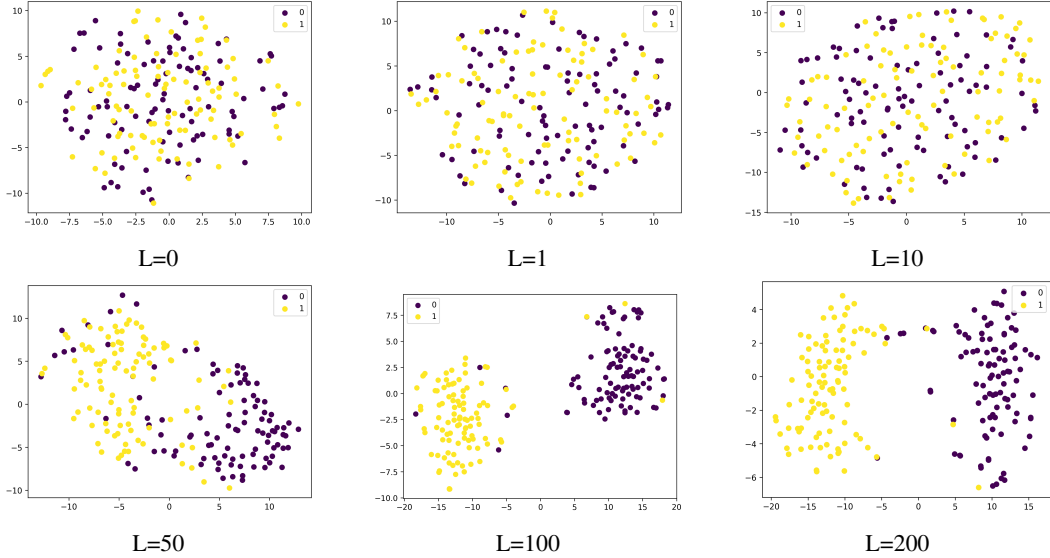


Figure 9: CSBM node features visualization. We update the features by Label-SBP.  $L$  is the propagation layer number. 0,1 represent different classes.

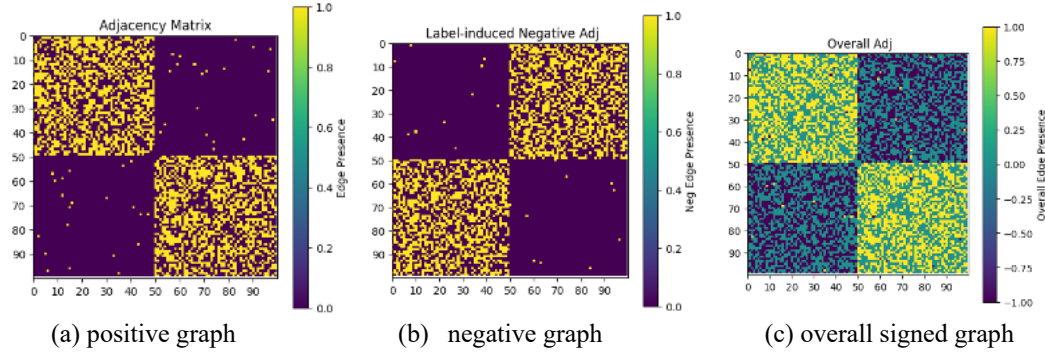


Figure 10: The visualization of the adjacency matrix of Label-SBP. Here left is the positive graph; middle is the negative graph; right is the overall signed graph.

prior methods by at least 10% and up to 30% points in GCN’s deepest layers, marking significant improvements. Moreover, unlike previous methods that perform best in shallow layers, SBP excels in moderately deep layers, as observed in GCN across all datasets. This further confirms the effectiveness of SBP.

### M.3.3 Repulsion ablation on heterophilic datasets

Our method SBP can outperform other baselines under  $\beta = 1$  across different layers, so we do not tune our hyper-parameters carefully. However, since  $\beta$  is the weight of the negative adjacency matrix (equation 4.3) representing the repulsion between different nodes, as seen in Figure 5 and 4, the best performance of SBP appears when  $\beta$  is larger in the heterophilic graphs, so the result in Figure 3a(a) is not the best performance of our SBP. To further show the effectiveness of our SBP, we conduct experiments on Cornell with different  $\beta$  in Table 11, the best  $\beta$  is 20 where the performance increases 25 points in deep layer 50.

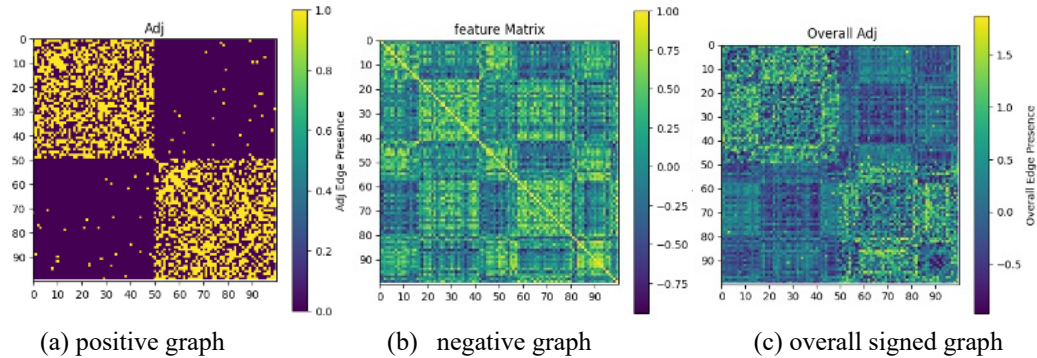


Figure 11: The visualization of the adjacency matrix of Feature-SBP. Here left is the positive graph; middle is the negative graph; right is the overall signed graph.

Table 9: CSBM test accuracy (%) comparison results. The best results are marked in blue on each layer. The second best results are marked in gray on each layer. We run 10 runs for the seed from 0 – 9 and demonstrate the mean  $\pm$  std in the table.

Model	#L=2	#L=5	#L=10	#L=20	#L=50	#L=100	#L=200
SGC	73.25 $\pm$ 6.90	44.50 $\pm$ 9.34	45.75 $\pm$ 9.36	45.75 $\pm$ 9.36	45.75 $\pm$ 9.36	45.75 $\pm$ 9.36	45.75 $\pm$ 9.36
Feature-SBP	48.75 $\pm$ 5.62	53.75 $\pm$ 6.45	63.75 $\pm$ 6.25	77.00 $\pm$ 5.45	82.00 $\pm$ 4.58	82.50 $\pm$ 5.12	82.00 $\pm$ 5.45
Label-SBP	85.75 $\pm$ 4.04	93.50 $\pm$ 4.06	93.50 $\pm$ 3.57	93.50 $\pm$ 3.57	92.25 $\pm$ 3.44	93.25 $\pm$ 3.72	91.25 $\pm$ 6.05

### M.3.4 Performance of SBP on more benchmarks

We further compare our SBP with SGC on six additional datasets [36] in Table 12. Our SBP outperforms SGC on five out of these six datasets. We believe that these six datasets, combined with the nine datasets presented in Table 15 of our paper, provide sufficient evidence to demonstrate the effectiveness of our approach.

### M.3.5 Combine SBP to other methods

In this paper, we focus on introducing a novel theoretic signed graph perspective for oversmoothing analysis, so we do not take many tricks into account or carefully fine-tune our hyperparameters. Thus, our results in the paper are not as comparable to previous baselines [9, 16, 31]. However, existing oversmoothing researches are indeed hard to compare, because they are often composed of multiple techniques — such as residual, BatchNorm, data augmentation — and the parameters are often heavily (over-)tuned on small-scale datasets. And it becomes clear that to attain SOTA performance, one needs to essentially compose multiple such techniques without fully understanding their individual roles. For example, GCNII uses both initial residual connection and identity map, further combined with dropout.

Our goal is to provide a new unified understanding of these techniques, so we justified it by showing that SBP as a single simple technique can attain good performance. And we believe that it would work complementarily with other techniques in the field, because oversmoothing is still challenging to solve with a very larger depth.

To further verify the effectiveness, we combine our SBP to one of the SOTA settings GCNII [9] and the results are as seen in Table 13. The results indicate that after combining our method, GCNII demonstrates greater robustness as the layers go deeper, particularly in the middle layers (layer=8), highlighting the efficacy of our signed graph insight.

### M.3.6 Performance of SBP on Large-scale graphs

We conducted experiments with a larger graph ogbn-products than ogbn-arxiv under 100 epochs and 2 layers in Table 14. The results indicate that our SBP outperforms the initial GCN baselines. Given



Table 10: GCN test accuracy (%) comparison results. The best results are marked in blue and the second best results are marked in gray on every layer. We run 5 runs for the seed from 0 – 4 and demonstrate the mean  $\pm$  std in the table.

Model	#L=2	#L=4	#L=8	#L=16	#L=32	#L=64
<i>Cora</i> [33]						
GCN [25]	80.68 $\pm$ 0.09	79.69 $\pm$ 0.00	74.32 $\pm$ 0.00	30.95 $\pm$ 0.00	30.95 $\pm$ 0.00	24.85 $\pm$ 7.46
GAT [43]	81.48 $\pm$ 0.48	80.69 $\pm$ 0.93	58.59 $\pm$ 1.95	25.17 $\pm$ 5.67	31.93 $\pm$ 0.21	28.38 $\pm$ 0.00
wGCN [17]	80.97 $\pm$ 0.28	80.51 $\pm$ 0.00	80.46 $\pm$ 1.77	70.53 $\pm$ 22.09	80.02 $\pm$ 0.12	27.90 $\pm$ 6.09
BatchNorm [24]	78.09 $\pm$ 0.00	77.87 $\pm$ 0.02	73.62 $\pm$ 0.57	70.79 $\pm$ 0.00	53.90 $\pm$ 2.19	35.32 $\pm$ 3.41
PairNorm [52]	79.01 $\pm$ 0.00	78.26 $\pm$ 0.50	73.21 $\pm$ 0.00	62.96 $\pm$ 0.00	48.13 $\pm$ 0.91	44.01 $\pm$ 3.46
ContraNorm [22]	81.55 $\pm$ 0.21	79.61 $\pm$ 0.75	77.71 $\pm$ 0.00	63.35 $\pm$ 0.00	44.56 $\pm$ 4.83	38.97 $\pm$ 0.00
DropEdge [37]	78.38 $\pm$ 0.00	74.47 $\pm$ 0.00	26.91 $\pm$ 0.83	22.24 $\pm$ 3.04	27.18 $\pm$ 0.00	25.98 $\pm$ 6.00
Residual	80.68 $\pm$ 0.09	78.77 $\pm$ 0.00	79.26 $\pm$ 0.21	40.91 $\pm$ 0.00	30.95 $\pm$ 0.00	27.90 $\pm$ 6.09
Feature-SBP	80.44 $\pm$ 0.83	79.26 $\pm$ 1.18	78.56 $\pm$ 0.59	77.22 $\pm$ 0.55	73.65 $\pm$ 0.48	61.62 $\pm$ 5.24
Label-SBP	80.31 $\pm$ 0.70	79.16 $\pm$ 1.30	79.50 $\pm$ 0.00	77.43 $\pm$ 1.49	74.52 $\pm$ 0.36	65.02 $\pm$ 2.97
<i>CiteSeer</i> [20]						
GCN [25]	67.45 $\pm$ 0.54	65.62 $\pm$ 0.25	37.22 $\pm$ 2.46	22.03 $\pm$ 4.76	19.65 $\pm$ 0.00	19.65 $\pm$ 0.00
GAT [43]	69.91 $\pm$ 0.86	67.47 $\pm$ 0.22	44.71 $\pm$ 3.07	23.48 $\pm$ 1.36	24.40 $\pm$ 0.40	25.95 $\pm$ 2.17
wGCN [17]	66.21 $\pm$ 0.63	66.49 $\pm$ 0.69	66.79 $\pm$ 0.00	57.54 $\pm$ 18.94	19.65 $\pm$ 0.00	19.65 $\pm$ 0.00
BatchNorm [24]	63.44 $\pm$ 0.94	62.34 $\pm$ 0.25	61.36 $\pm$ 0.00	50.58 $\pm$ 1.24	41.41 $\pm$ 0.00	35.00 $\pm$ 1.09
PairNorm [52]	63.58 $\pm$ 0.63	64.32 $\pm$ 0.95	61.95 $\pm$ 1.24	50.06 $\pm$ 0.00	37.21 $\pm$ 1.87	36.09 $\pm$ 0.07
ContraNorm [22]	66.83 $\pm$ 0.49	64.78 $\pm$ 0.92	60.70 $\pm$ 0.60	44.79 $\pm$ 1.65	37.36 $\pm$ 0.25	30.85 $\pm$ 0.81
DropEdge [37]	63.86 $\pm$ 0.03	62.24 $\pm$ 0.90	24.73 $\pm$ 5.72	20.65 $\pm$ 0.00	20.04 $\pm$ 0.19	19.95 $\pm$ 0.09
Residual	67.45 $\pm$ 0.54	66.21 $\pm$ 0.16	67.34 $\pm$ 0.00	33.21 $\pm$ 0.00	19.65 $\pm$ 0.00	19.65 $\pm$ 0.00
Feature-SBP	67.38 $\pm$ 0.66	66.94 $\pm$ 0.00	66.29 $\pm$ 0.02	65.35 $\pm$ 1.99	61.43 $\pm$ 0.00	42.09 $\pm$ 1.65
Label-SBP	67.23 $\pm$ 0.64	66.72 $\pm$ 0.00	66.29 $\pm$ 0.89	65.50 $\pm$ 2.13	59.93 $\pm$ 0.85	44.41 $\pm$ 1.57
<i>PubMed</i> [6]						
GCN [25]	76.44 $\pm$ 0.34	76.52 $\pm$ 0.32	69.58 $\pm$ 5.89	39.92 $\pm$ 0.00	39.92 $\pm$ 0.00	39.92 $\pm$ 0.00
+BatchNorm [24]	75.52 $\pm$ 0.12	77.15 $\pm$ 0.00	77.10 $\pm$ 0.00	76.92 $\pm$ 0.00	75.43 $\pm$ 0.00	69.33 $\pm$ 1.01
+PairNorm [52]	75.66 $\pm$ 0.11	76.71 $\pm$ 0.00	77.99 $\pm$ 0.00	77.22 $\pm$ 0.39	75.52 $\pm$ 2.02	71.22 $\pm$ 3.68
+ContraNorm [22]	76.05 $\pm$ 0.33	78.42 $\pm$ 0.00	OOM	OOM	OOM	OOM
+DropEdge [37]	73.41 $\pm$ 0.03	73.96 $\pm$ 0.79	52.51 $\pm$ 10.91	40.27 $\pm$ 0.00	39.90 $\pm$ 0.59	40.08 $\pm$ 0.39
+Residual	76.44 $\pm$ 0.34	77.28 $\pm$ 0.00	77.38 $\pm$ 0.00	63.14 $\pm$ 3.05	39.92 $\pm$ 0.00	39.92 $\pm$ 0.00
Feature-SBP	75.72 $\pm$ 0.06	76.84 $\pm$ 0.00	78.39 $\pm$ 0.00	79.71 $\pm$ 0.00	77.59 $\pm$ 0.23	78.06 $\pm$ 0.13
Label-SBP	76.33 $\pm$ 0.25	76.91 $\pm$ 0.00	77.60 $\pm$ 0.49	76.31 $\pm$ 0.00	77.17 $\pm$ 0.67	78.01 $\pm$ 0.16

Table 11: Ablation study of negative weight  $\beta$  on Cornell dataset.

Layer	2	5	10	20	50
$\beta = 0.1$	72.97 $\pm$ 0.00	67.57 $\pm$ 0.00	51.53 $\pm$ 0.00	35.14 $\pm$ 0.00	29.73 $\pm$ 0.00
$\beta = 1$ (default)	72.97 $\pm$ 0.00	67.57 $\pm$ 0.00	51.53 $\pm$ 0.00	45.95 $\pm$ 0.00	35.14 $\pm$ 0.00
$\beta = 10$	70.27 $\pm$ 0.00	67.57 $\pm$ 0.00	58.11 $\pm$ 1.35	51.53 $\pm$ 0.00	51.53 $\pm$ 0.00
$\beta = 20$ (best)	70.27 $\pm$ 0.00	70.27 $\pm$ 0.00	67.57 $\pm$ 0.00	59.46 $\pm$ 0.00	59.46 $\pm$ 0.00
$\beta = 50$	64.60 $\pm$ 0.00	40.54 $\pm$ 0.00	40.54 $\pm$ 0.00	40.54 $\pm$ 0.00	40.54 $\pm$ 0.00

the results presented for ogbn-arxiv in Table 5 of our paper, we believe these findings adequately demonstrate the performance of our SBP on large-scale graphs.

### M.3.7 Further Optimization based on SBP

Based on the experiment results, we want to propose 2 strategies for further optimization.

Table 12: Performance Comparison on more datasets

	actor	penny94	roman-empire	Tolokers	Questions	Minesweeper
SGC	29.18 $\pm$ 0.10	72.56 $\pm$ 0.05	40.83 $\pm$ 0.03	78.18 $\pm$ 0.02	97.09 $\pm$ 0.00	80.43 $\pm$ 0.00
Feature-SBP	34.93 $\pm$ 0.02	75.68 $\pm$ 0.01	66.48 $\pm$ 0.02	78.24 $\pm$ 0.04	97.14 $\pm$ 0.02	80.00 $\pm$ 0.00
Label-SBP	34.94 $\pm$ 0.00	75.74 $\pm$ 0.01	66.32 $\pm$ 0.01	78.46 $\pm$ 0.08	97.15 $\pm$ 0.02	80.00 $\pm$ 0.00

Table 13: Performance Comparison between SBP and GCNII under the GCNII settings on Cora and Citesser datasets

		2	4	8	16	32	64
Cora	GCNII	78.58 ± 0.00	77.76 ± 0.24	73.47 ± 3.82	78.12 ± 1.32	82.54 ± 0.00	81.34 ± 0.53
	Label-SBP	78.74 ± 1.54	78.87 ± 0.00	79.14 ± 0.35	79.17 ± 0.41	80.86 ± 0.32	81.38 ± 0.30
	Feature-SBP	77.95 ± 0.91	78.82 ± 0.00	78.11 ± 1.62	78.82 ± 0.29	81.82 ± 0.47	81.65 ± 0.40
Citesser	GCNII	61.66 ± 0.67	63.23 ± 2.31	64.58 ± 2.66	66.21 ± 0.64	69.38 ± 0.83	69.73 ± 0.26
	Label-SBP	65.31 ± 0.63	63.93 ± 3.66	68.33 ± 0.99	66.46 ± 0.00	70.00 ± 0.81	69.47 ± 0.25
	Feature-SBP	65.63 ± 0.87	64.43 ± 3.55	68.44 ± 1.19	66.94 ± 0.00	69.98 ± 0.93	69.66 ± 0.28

Table 14: Performance of different models on ogbn-products dataset. Time means the runtime, the format is (hour: minutes: seconds).

Method	Accuracy	Time
GCN	73.96	00:06:33
BatchNorm	74.93	00:06:18
Feature-SBP	74.90	00:06:43
Label-SBP	76.62	00:06:39

1) hyper-parameter tuning on the negative weight  $\beta$ . As seen in Figures 5 and 4, we found that  $\beta$  influences the performance a lot, our default  $\beta = 1$  for Table 15 and 4 is certainly not optimal for the above 4 homophilic datasets. We suggest tuning higher  $\beta$  for the heterophilic graphs since they need more repulsion and smaller for the homophilic datasets. As the layer deepens, maybe greater weight should be placed on the negative adjacency graphs to alleviate oversmoothing.

2) adapt our SBP to more effective GNNs. Our method is simple, architecture-free, without additional learnable parameters, and thus can be flexibly applied in various architectures. As seen in Appendix M.3.5, we adapt our SBP to the GCNII models, and the results increase more than adaptation in vanilla GNN as shown in Table 15 and 4. Besides, compared to the GCNII, our SBP is more robust and stable to the layers as seen in Table 13.

Table 15: SGC test accuracy (%) comparison results. The best results are marked in blue and the second best results are marked in gray on every layer. We run 10 runs and demonstrate the mean  $\pm$  std in the table.

Model	#L=2	#L=5	#L=10	#L=20	#L=50	#L=100	#L=300
<i>Cora</i> [33]							
SGC	80.21 $\pm$ 0.07	81.45 $\pm$ 0.14	81.53 $\pm$ 0.19	79.53 $\pm$ 0.14	79.20 $\pm$ 0.21	76.13 $\pm$ 0.24	65.64 $\pm$ 1.15
+BatchNorm	77.90 $\pm$ 0.00	78.02 $\pm$ 0.04	76.94 $\pm$ 0.08	75.18 $\pm$ 0.09	74.54 $\pm$ 0.05	72.64 $\pm$ 0.05	63.12 $\pm$ 0.06
+PairNorm	80.30 $\pm$ 0.05	78.57 $\pm$ 0.00	78.14 $\pm$ 0.07	76.90 $\pm$ 0.00	77.49 $\pm$ 0.03	72.01 $\pm$ 0.03	40.93 $\pm$ 0.11
+ContraNorm	81.60 $\pm$ 0.00	80.67 $\pm$ 0.06	79.11 $\pm$ 0.03	74.28 $\pm$ 0.15	69.67 $\pm$ 1.23	65.58 $\pm$ 2.11	47.21 $\pm$ 10.80
+DropEdge	73.58 $\pm$ 2.76	62.11 $\pm$ 5.10	39.21 $\pm$ 7.54	15.07 $\pm$ 6.22	11.16 $\pm$ 2.73	11.15 $\pm$ 2.81	11.15 $\pm$ 2.81
+Residual	77.81 $\pm$ 0.03	81.47 $\pm$ 0.05	82.90 $\pm$ 0.00	79.87 $\pm$ 0.05	75.64 $\pm$ 0.05	66.90 $\pm$ 0.10	25.33 $\pm$ 0.46
Feature-SBP	78.10 $\pm$ 0.11	80.88 $\pm$ 0.23	80.83 $\pm$ 0.37	82.46 $\pm$ 0.07	80.47 $\pm$ 0.25	80.23 $\pm$ 0.51	77.49 $\pm$ 0.23
Label-SBP	81.14 $\pm$ 0.49	82.90 $\pm$ 0.00	82.54 $\pm$ 0.05	82.44 $\pm$ 0.05	82.60 $\pm$ 0.00	81.10 $\pm$ 0.00	74.98 $\pm$ 0.11
<i>CiteSeer</i> [20]							
SGC	71.88 $\pm$ 0.27	72.55 $\pm$ 0.25	72.53 $\pm$ 0.15	72.07 $\pm$ 0.21	69.83 $\pm$ 0.20	65.42 $\pm$ 0.43	54.69 $\pm$ 0.98
+BatchNorm	60.85 $\pm$ 0.09	60.45 $\pm$ 0.07	61.74 $\pm$ 0.27	63.29 $\pm$ 0.18	63.71 $\pm$ 0.18	64.28 $\pm$ 0.27	59.42 $\pm$ 0.20
+PairNorm	70.83 $\pm$ 0.06	69.68 $\pm$ 0.32	70.54 $\pm$ 0.04	69.86 $\pm$ 0.08	70.51 $\pm$ 0.07	69.86 $\pm$ 0.06	65.22 $\pm$ 0.16
+ContraNorm	72.25 $\pm$ 0.08	71.9 $\pm$ 0.06	71.52 $\pm$ 0.04	59.82 $\pm$ 2.30	52.87 $\pm$ 1.86	45.93 $\pm$ 1.40	35.67 $\pm$ 1.62
+DropEdge	65.63 $\pm$ 1.76	51.80 $\pm$ 4.61	25.36 $\pm$ 2.54	18.60 $\pm$ 3.78	16.52 $\pm$ 3.97	16.49 $\pm$ 4.03	16.49 $\pm$ 4.03
+Residual	71.61 $\pm$ 0.17	72.31 $\pm$ 0.15	72.78 $\pm$ 0.12	72.50 $\pm$ 0.14	71.24 $\pm$ 0.21	69.85 $\pm$ 0.22	62.11 $\pm$ 0.42
Feature-SBP	70.63 $\pm$ 0.52	70.85 $\pm$ 0.09	70.52 $\pm$ 0.14	70.76 $\pm$ 0.22	68.25 $\pm$ 0.46	67.20 $\pm$ 1.15	65.12 $\pm$ 1.95
Label-SBP	72.01 $\pm$ 0.10	72.87 $\pm$ 0.05	72.72 $\pm$ 0.28	73.04 $\pm$ 0.10	72.52 $\pm$ 0.17	72.45 $\pm$ 0.11	70.97 $\pm$ 0.22
<i>PubMed</i> [6]							
SGC	76.99 $\pm$ 0.38	75.92 $\pm$ 0.30	76.18 $\pm$ 0.70	77.13 $\pm$ 0.34	76.09 $\pm$ 0.43	76.19 $\pm$ 0.19	70.58 $\pm$ 0.52
+BatchNorm	77.15 $\pm$ 0.09	77.87 $\pm$ 0.05	78.47 $\pm$ 0.05	77.90 $\pm$ 1.10	76.85 $\pm$ 0.08	74.35 $\pm$ 0.08	69.61 $\pm$ 0.08
+PairNorm	77.69 $\pm$ 0.26	75.78 $\pm$ 0.37	75.13 $\pm$ 0.13	74.75 $\pm$ 0.33	72.13 $\pm$ 0.11	69.79 $\pm$ 0.16	71.75 $\pm$ 0.51
+ContraNorm	79.30 $\pm$ 0.10	78.69 $\pm$ 0.07	77.54 $\pm$ 0.09	73.67 $\pm$ 0.12	71.37 $\pm$ 3.15	67.96 $\pm$ 3.24	65.00 $\pm$ 4.12
+DropEdge	74.64 $\pm$ 1.37	69.83 $\pm$ 3.19	60.28 $\pm$ 2.70	32.62 $\pm$ 10.95	33.95 $\pm$ 10.44	33.95 $\pm$ 10.44	33.95 $\pm$ 10.44
+Residual	77.40 $\pm$ 0.06	79.30 $\pm$ 0.10	79.83 $\pm$ 0.09	79.44 $\pm$ 0.09	74.96 $\pm$ 0.09	71.72 $\pm$ 0.13	55.57 $\pm$ 0.21
Feature-SBP	73.99 $\pm$ 1.44	74.36 $\pm$ 0.63	75.61 $\pm$ 0.24	77.09 $\pm$ 0.35	77.41 $\pm$ 0.21	77.10 $\pm$ 0.36	76.87 $\pm$ 0.49
Label-SBP	78.98 $\pm$ 0.14	80.14 $\pm$ 0.05	80.22 $\pm$ 0.04	80.32 $\pm$ 0.04	80.20 $\pm$ 0.00	79.60 $\pm$ 0.00	73.96 $\pm$ 0.05